Florian Bloder

Impact of nebulizer atomization techniques on stability and transport efficiency of liposomal formulations

Master's thesis

Institute of Medical Engineering
Graz University of Technology
Kronesgasse 5, A - 8010 Graz

Supervisor: Assoz. Prof.^{in} Univ.-Doz.^{in} Dr.^{in} Ruth Prassl
Evaluator: Univ.-Prof. Dipl.-Ing. Dr.techn. Rudolf Stollberger

Graz, February 24, 2014

Ludwig Boltzmann Institute for Lung Vascular Research
Center for Medical Research
Stiftingtalstrasse 24, A - 8010 Graz

STATUTORY DECLARATION

I declare that I have authored this thesis independently, that I have not used other than the declared sources / resources, and that I have explicitly marked all material which has been quoted either literally or by content from the used sources.

Graz, February 24, 2014

Zusammenfassung

Liposomen sind vielversprechende Wirkstoffträgersysteme für die inhalative Verabreichung von Medikamenten mit Verneblern.

Ziel dieser Arbeit war es die unterschiedlichen Verneblerprinzipien auf ihre Anwendbarkeit für liposomale Formulierungen zu untersuchen.

Ein Ultraschallvernebler, ein Düsenvernebler und ein Meshvernebler wurden miteinander verglichen. Drei liposomale Formulierungen mit unterschiedlichen Oberflächeneigenschaften wurden getestet. Die Hauptlipide der drei Formulierungen waren Dipalmitoylphosphocholin und Cholesterin.
Der Einfluss der Vernebelung auf Teilchengröße, Lipidkonzentration und Intaktheit der liposomalen Formulierungen wurde untersucht. Die Intaktheit wurde mittels eines Fluorophor-Quencher Systems ermittelt. Weiters wurde die Aerosolpartikelgröße der Vernebler bestimmt sowie die Intaktheit der Liposomen in Lungen-Surfactant.

Es zeigte sich, dass die Stabilität der Liposomen während der Vernebelung hauptsächlich von der liposomalen Formulierung abhängt. Die Liposomen sind umso stabiler je weniger ihre Oberfläche modifiziert wird. Im Gegensatz dazu hängt die Transporteffizienz von dem Verneblertyp ab und ist für alle Formulierungen ähnlich. Die Mesh-Technologie ist die effizienteste Vernebelungsmethode. Sowohl die Aerosolpartikelgröße als auch die Stabilität in Lungen-Surfactant sind unabhängig von der liposomalen Formulierung.

Alles in allem ist die Mesh-Technologie die beste Vernebelungsmethode und geeignet für oberflächenunmodifizierte Liposomen bestehend aus Dipalmitoylphosphocholin und Cholesterin.

Schlüsselwörter: Vernebler, Liposom, Inhalation, Tröpfchengröße, Stabilität

Abstract

Liposomes are a promising drug carrier system for inhalations with a nebulizer.

Aim of this study was to examine different nebulizer principles on their applicability for the transport of liposomes.

An ultrasonic nebulizer, an air-jet nebulizer, and a vibrating mesh nebulizer were compared. Three liposomal formulations with different surface properties were tested. The main lipids of the three formulations were dipalmitoylphosphocholin and cholesterol.
The influence of nebulization on particle size, lipid concentration, and integrity of the liposomal formulations was determined. The integrity of liposomes was investigated with a fluorophore-quencher system. Furthermore the aerosol particle size of the nebulizers and the integrity of liposomes in lung-surfactant were examined.

It turned out that the stability of liposomes during nebulization depends mainly on the liposomal formulation. The less liposomes are surface modified the higher is their stability. In contrast transport efficiency depends on the applied nebulizer type. The vibrating mesh technique is most efficient. Both, aerosol particle size and stability of liposomes in lung surfactant are independent of the liposomal formulation.

Taken together, the vibrating mesh technique is the best nebulization method and suitable for surface-unmodified liposomes consisting of dipalmitoylphosphocholin and cholesterol.

Key words: nebulizer, liposome, inhalation, droplet size, leakage

Acknowledgements

I thank Regina Leber, who was my main contact person for discussions and questions.
I thank Bernhard Lehofer for his help and tutoring when I started my work.
I thank Ruth Prassl for her remarks and explanations.
I thank Leigh Marsh for our fruitful discussions.

I thank Caroline, Christian, Dagmar, Gebhard, Hans, Karin, Kerstin, Nermina, Pritesh, and Sabrina for technical support and a great place to work.

All experiments were done at the IBN[1]. Exceptions are the ζ-potential and particle size measurements which were done at the Karl-Franzens-University Graz with thankworthy technical support from Bettina Bauer.

The author was employed and funded for six months by the Ludwig Boltzmann Institute for Lung Vascular Research.

[1]Institute of Biophysics and Nanosystems Research

Contents

Abbreviations

ANOVA	analysis of variance
ANTS	8-aminophtalene-1,3,6-trisulfonic acid disodium salt
CF	5(6)-carboxyfluorescein
DOTAP	N-[1-(2,3-dioleoyloxy)propyl]-N,N,N-trimethylammonium methyl-sulfate
DPI	dry powder inhaler
DPPC	1,2-dipalmitoyl-sn-glycero-3-phosphocholine
DPPE–PEG_{2000}	1,2-dipalmitoyl-sn-glycero-3-phosphoethanolamine-N-[methoxy(polyethyleneglycol)-2000]
DPX	p-xylene-bis-pyridinium bromide
F1	formulation 1
F2	formulation 2
F3	formulation 3
HEPES	2-(4-(2-hydroxyethyl)- 1-piperazinyl)-ethansulfonicacid
MMAD	mass median aerodynamic diameter
MMD	mass median diameter
PC	phosphatidylcholine
PDI	polydispersity index
PEGylation	polyethylene glycol conjugation
pMDI	pressured metered-dose inhaler
SD	standard deviation
SP-A	surfactant apoprotein A
SP-B	surfactant apoprotein B
SP-C	surfactant apoprotein C
TBHBA	2,4,6-tribromo-3-hydroxybenzoic acid, uric acid
TRIS	tris(hydroxymethyl)aminomethane

Symbols

α	significance level
α'	significance level with Bonferroni correction ($\alpha/3$)
χ	mole fraction
χ_{DPPC}	mole fraction of DPPC
χ_{lipid}	mole fraction of the lipid
γ	surface tension
η	viscosity
λ_{D}	Debye length
ρ	density of the drop
ζ	zeta

c_{DPPC}	concentration of DPPC
C_{e}	static capacity between the main electrode and the substrate electrode of the piezoelectric element
$c_{\mathrm{i\_total}}$	total molar concentration
C_{m}	capacity in the electric equivalent circuit of the piezoelectric element
c_{NaCl}	concentration of NaCl
c_{s}	lipid concentration at the start
c_{standard}	PC concentration of the standard
c_{t}	lipid concentration in aerosol or remainder
c_{total}	total lipid concentration
$c_{\mathrm{phospholipids}}$	phospholipid concentration
$d(0.1)$	diameter, 10% of the mass is in particles with a smaller diameter
$d(0.5)$	diameter, 50% of the mass is in particles with a smaller diameter
$d(0.9)$	diameter, 90% of the mass is in particles with a smaller diameter
e	elementary charge
e_{r}	relative permittivity of the solution
e_{o}	permittivity of vacuum
g	gravitational acceleration
h	thickness of active layer in the actuator
h'	thickness of reaction layer in the actuator
I_{s}	fluorescence intensity before nebulization without Triton X-100™
I_{S}	fluorescence intensity before nebulization with Triton X-100™
I_{t}	fluorescence intensity of aerosol/remainder without Triton X-100™
I_{T}	fluorescence intensity of aerosol/remainder with Triton X-100™

k	Boltzmann constant
L_1	inductivity which is parallel to the piezoelectric element, determines the resonance mode
l	length of a tube
L_m	inductivity in the electric equivalent circuit of the piezoelectric element
m	mass
m_total	mass of all lipids together
m_lipid	mass of the lipid
M	molar mass
M_DPPC	molar mass of DPPC
M_lipid	molar mass of the lipid
M_total	total molar mass
p	p-value
p'	p-value, one sided
ΔP	pressure drop
Q	flow rate
r	radius of a tube/vessel
R	radius of sphere
R_m	resistor in the electric equivalent circuit of the piezoelectric element
T	absolute temperature
V_d	volume of the drop
w	mass fraction
w_lipid	mass fraction of the lipid
Y	elastic modulus of active layer in the actuator
Y'	elastic modulus of reaction layer in the actuator

List of Figures

List of Tables

1 General Introduction

1.1 Liposomes

A liposome is a vesicle composed of a lipid bilayer (figure 1a), derived from the greek words lipo „fat“ and soma „body“. Liposomes are self-assembling structures of amphipathic lipids in aqueous environments. These lipids have a hydrophilic head and a hydrophobic tail. It is energetically favorable that the hydrophobic tails attach to each other building lipid bilayers. These bilayers further decrease free energy by building closed structures. Liposomes can consist of one lipid bilayer (unilamellar vesicles) or multiple lipid bilayers (multilamellar vesicles) [1].

Within the lipid bilayer, which is a thin membrane, lipid molecules can diffuse freely (figure 1b). Fluidity and permeability of the bilayer depend on temperature and lipid composition. If the Van-der-Waals interactions between the lipids are low, molecules can diffuse more freely. Interactions between molecules might be lowered with shorter hydrocarbon chains. Another possibility is a cis-double bond causing a kink in the tail, which decreases the packing tightness. At a given temperature (the phase transition temperature) the fluid bilayer of a single type of phospholipid changes from a fluid phase to a rigid, gel phase [2].

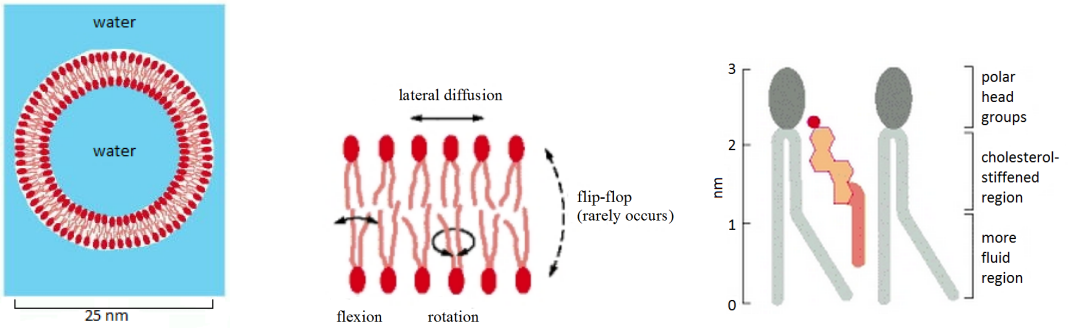

(a) Schematic presentation of a liposome.

(b) Possible movements of a single lipid molecule in a lipid bilayer.

(c) Cholesterol in a lipid (bi-)layer.

Figure 1: Liposome structure, bilayer fluidity, and inclusion of cholesterol. All pictures are taken from [2].

When cholesterol is added to lipid bilayers, the steroid rings interact with parts of the hydrocarbon chains of the other lipids. This decreases permeability for small, polar molecules [2]. Figure 1c shows a schematic drawing of a cholesterol molecule interacting with two

phospholipid molecules in one monolayer of a lipid bilayer.

Liposomes are a promising drug delivery system, due to their biocompatibility and fluidity properties which can be modified easily. So far, there are about 12 approved liposome-based drugs. Most of them are for intravenous injection. Over 21 liposome-based drugs are in clinical trials [3]. Two of them, Arikace®[3] and Pulmaquin™[4], are made for portable aerosol delivery.

In this study the influence of a surface coat with poly-ethylene glycol (PEG) and the influence of a positive surface charge, by inclusion of a cationic lipid, on liposome stability during nebulization were examined. Three different liposomal formulations were nebulized.
The first liposomal formulation (F1) consisted of 1,2-dipalmitoyl-sn-glycero-3-phosphocholine (DPPC) and cholesterol.
The second liposomal formulation (F2) contained similar mole ratios of DPPC and cholesterol as F1. Additionally F2 contained small portions of 1,2-dipalmitoyl-sn-glycero-3-phosphoethanolamine-N-[methoxy(polyethyleneglycol)-2000] (DPPE--PEG_{2000}).
The third liposomal formulation (F3) contained the same lipids as F2 and N-[1-(2,3-dioleoyloxy)propyl]-N,N,N-trimethylammonium methyl-sulfate (DOTAP) additionally. The detailed composition of each formulation is shown in the methods section (see chapter 2.3.3).
Note: PEGylation is widely used in other studies, because among other things it reduces liposome uptake by macrophages [5]. DOTAP is often used as a transfection reagent [6].

1.2 The fluorophore/quencher system ANTS/DPX

In order to determine liposome stability during nebulization, a fluorescence leakage assay was performed. The fluorophore/quencher system consisting of the polyanionic fluorophore 8-aminophtalene-1,3,6-trisulfonic acid disodium salt (ANTS) and its cationic quencher p-xylene-bis-pyridinium bromide (DPX) was applied numerous times for leakage measurements in previous studies [7–15]. Both, ANTS and DPX were enclosed inside the liposomes during preparation. The principle is as follows (figure 2):
After liposome preparation and separation from non - encapsulated ANTS and DPX molecules, all ANTS and DPX molecules are enclosed in liposomes, depicted in (a). The black annular structure symbolizes the liposome. When ANTS and DPX molecules are in close proximity (inside the liposomes), fluorescence is quenched by collision. Hardly any fluorescence is being detected.

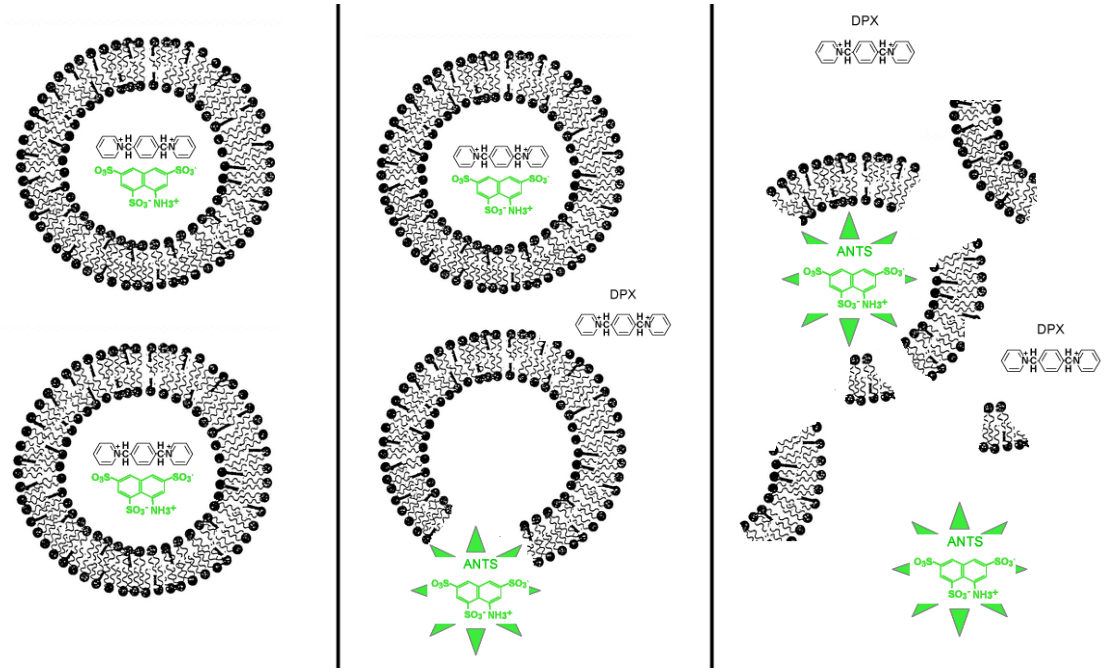

(a) after preparation (b) upon membrane leakage (c) Triton X-100™ added

Figure 2: Principle of the ANTS/DPX leakage assay. The picture was drawn with elements from [16, 17].

Upon membrane leakage, some ANTS and DPX molecules are released, depicted in (b). Distance between free fluorophore and its free quencher increase in solution, hence collisional fluorescence quenching is reduced and more fluorescence can be detected.
Triton X-100™ is a detergent which destroys lipid bilayers. If added to liposomes all ANTS and DPX molecules are released (c).

1.3 Inhalers

1.3.1 Overview: pMDIs, DPIs, and nebulizers

Pulmonary drug delivery is usually achieved by inhalation through the mouth [18] and used to treat local, pulmonary diseases (for example COPD[2], asthma) or systematic diseases (for example diabetes). The advantages of pulmonary drug delivery are the rapid uptake and action, because of a huge permeable surface area of 80-140 m^2 in the lungs. Lower doses can be applied compared to an administration to the gastrointestinal tract,

[2]Chronic Obstructive Pulmonary Disease

due to less enzymatic degradation. Moreover the hepatic first pass effect, that is degradation by the liver, is reduced. One disadvantage is that frequent administrations are necessary, due to the rapid removal and action [19].

For drug administration to the respiratory tract pressured metered-dose inhalers (pMDIs), dry powder inhalers (DPIs) or nebulizers are being used. The following explanations clarify the differences among those devices.

pMDI. A pMDI, shown in figure 3, gives a single burst, when pushed by the patient.

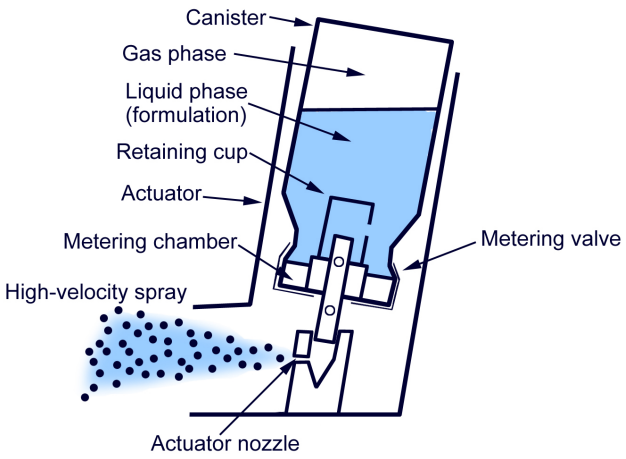

Figure 3: The principle of a pMDI. The container, often made of aluminum, withstands high pressures from inside. In rest, a channel between fluid and metered chamber is open. When the pMDI is activated, the canister is pressed down, this channel closes and the channel to the expansion chamber and actuator nozzle opens. The plastic actuator surrounds everything and is for the use of the patient [20].

Usually there is no burst counter and pMDIs are sold with the medicine proprietarily inside. Medicine is suspended or dissolved in propellants. Propellants are liquefied compressed gases and needed to provide the force to generate an aerosol cloud. pMDIs are wide spread because they are cheap [21].

DPI. DPIs contain a dry powder without propellants. Instead some formulations contain lactose. The powder is sold proprietarily inside the DPI or manually loaded. The energy from the patient's inhalation disaggregates the powder into smaller particles. Since

a strong air flow from the patient is needed, DPIs are usually not used with small children [22].

Nebulizers. A nebulizer is a medical device that converts a liquid into aerosol droplets (suitable for inhalation) [18]. Nebulizers have to be loaded before treatment. Compared to pMDIs and DPIs they need a longer time to generate the aerosol. In return the delivered dose is more precise. Nebulizers are used for very high doses of bronchodilators, special combinations of medicaments or when the patients breathing pattern is inappropriate for other devices (small children, severe asthma) [22]. Nebulizers are expensive and have an electric power supply. There are three technologies for aerosol generation. According to these principles, nebulizers are categorized as „air-jet“, „ultrasonic“ or „vibrating mesh“ [23].

1.3.2 Air-jet nebulizers

Air-jet nebulizers press air or oxygen through a pipe with a very narrow hole, known as a Venturi. At the Venturi the velocity of gas is very high and thus pressure falls, depicted in figure 4.

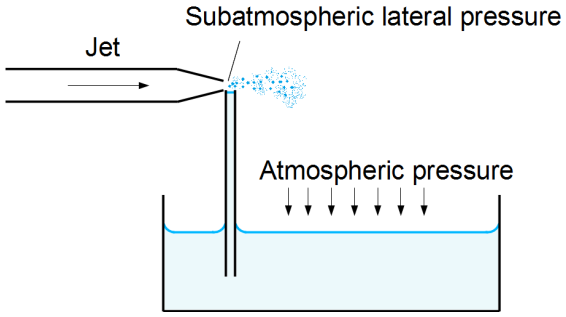

Figure 4: Schematic presentation of the air-jet principle to generate aerosol [24].

The negative lateral pressure causes the liquid to rise in the capillary tube according to the Bernoulli effect. The high kinetic energy of the gas flow immediately breaks up the liquid into an aerosol [24].
A baffle is used to exclude droplets which are too large for inhalation. The air-flow is provided with a compressor. Some air-jet nebulizers use the negative pressure of the air flow to suck in air through an open vent (hole) at the top and thus enhance airflow [25]. The air-jet principle reduces temperature of the liquid during nebulization. On one hand this is due to the evaporation of the fluid. It saturates the gas used to generate the aerosol. On the other hand a decrease in temperature is caused by adiabatic expansion

of the generating gas [26].
The applied air-jet in this study was the MicroDrop MasterJet® (MPV Truma, Putzbrunn, Germany).

1.3.3 Ultrasonic nebulizers

In an ultrasonic nebulizer a piezoelectric crystal is in contact with the fluid. An alternating voltage is applied which causes the crystal to change its size. This size change causes a longitudinal, mechanical wave in the liquid. Capillary waves evolve on the liquid surface due to cavitation, acoustic streaming and/or other mechanisms. Droplets are pinched off and ejected at the peaks of the waves. The droplet diameter is proportional to the wavelength of the capillary waves. The wavelength is influenced by the actuation frequency and properties of the liquid. Higher frequencies lead to smaller droplets. Frequencies are limited to approximately 3 MHz due to resonance modes and limits of the piezoelectric crystal [27]. Once again a baffle is used to retain droplets which are too large.
Figure 5 shows a collapsing cavitation bubble which leads to the excitation of a capillary wave.

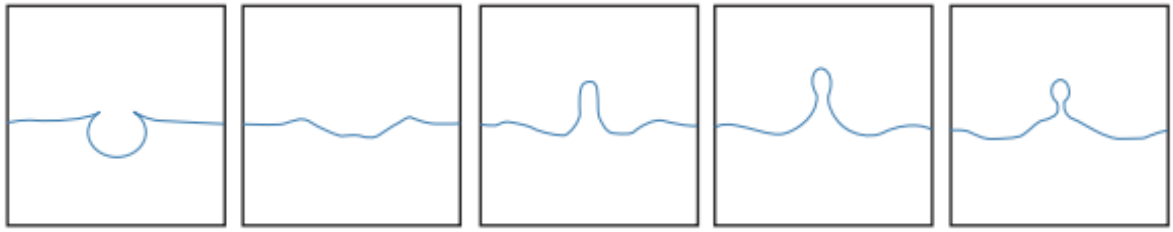

Figure 5: Schematic illustration of a cavitation bubble near the interface. The rim of the collapsing bubble is stretched outwards, radially downward and subsequently inwards. Eventually an aerosol droplet is pinched off from the capillary wave. (from left to right) [27].

The ultrasonic waves cause the liquid to heat up during nebulization. This is why newer ultrasonic nebulizers use a contact fluid, usually water, between piezoelectric element and medication [28].

The applied ultrasonic nebulizer in this study was the Optineb®-ir (Nebu-Tec, Elsenfeld, Germany). This nebulizer operates at a frequency of 1.6 MHz. A schematic presentation of the Optineb®-ir is shown in figure 6.

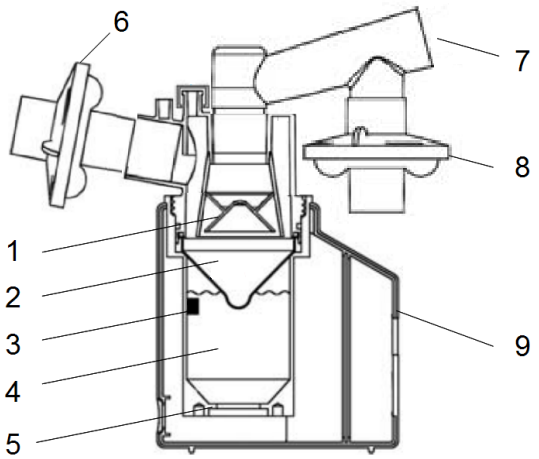

Figure 6: Schematic illustration of the Optineb®-ir. Elements of this picture were taken from [29].

#1 is the baffle plate. In this study a „blue“ (MMAD: 3.2 µm for Ventavis[3], see chapter 3.2 for an explanation of the MMAD) baffle plate from Nebu-Tec was used. Different baffle plates should yield to different aerosol droplet sizes. #2 is a disposable medicine cup, which should be undeformed at the apex. #3 is a sensor, which detects if the contact fluid chamber is filled with (distilled) water or not. #4 is the contact fluid chamber. #5 is the piezoelectric element. #6 is the inhalation filter. #7 leads to the mouth piece (not shown). #8 is the exhalation filter. #9 are display and the operating buttons.

1.3.4 Vibrating mesh nebulizers

The vibrating mesh principle is the latest principle. Vibrating mesh nebulizers are popular because they are small, quiet, and have the highest aerosol output per time [28]. During nebulization there is just a slight increase in temperature in the remaining fluid.

Principle. The centerpiece of vibrating mesh nebulizers is a perforate membrane. For example a metallic plate with conical holes. Due to vibrations of the plate, the adjacent fluid is pressed through the holes of the plate, as shown in figure 7.
A special application of the vibrating mesh principle is the „passive“ vibrating mesh. In this case the piezoelectric crystal is connected to the liquid with a transducer horn. The liquid is pressed through a static mesh, due to ultrasonic waves [28].

[3]A medicine which is used to treat pulmonary arterial hypertension

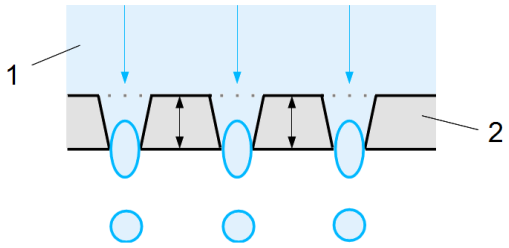

Figure 7: Working principle of the vibrating-mesh nebulizer. In the figure three apertures out of several thousand are shown. #1 is the fluid which is pressed through the vibrating membrane (#2). Redrawn from [30].

Nebulizer structure. A schematic presentation of an active vibrating mesh nebulizer is given in figure 8.

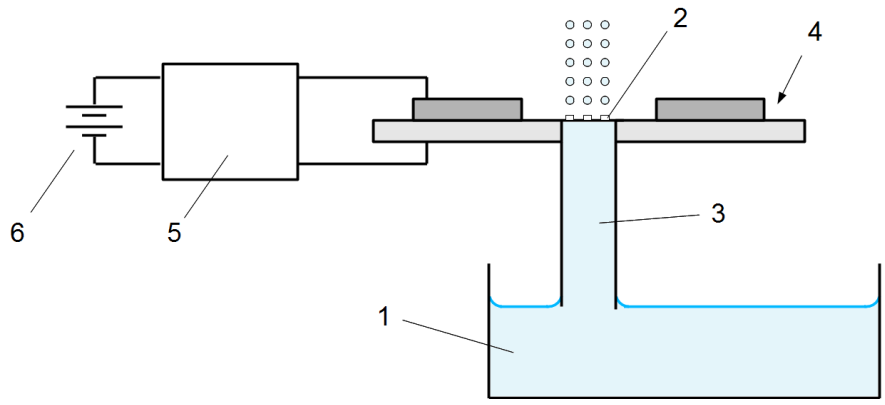

Figure 8: Schematic presentation of a vibrating mesh nebulizer. Redrawn from [31].

The fluid source (#1) of the nebulizer might be directly attached to the perforate membrane (#2). Alternatively the fluid might be brought by a capillary feed (#3) to the perforate membrane. The membrane might be vibrated with an annular piezoelectric disc (#4). This disc (actuator) is operated by an electronic circuit (#5) which receives its power from a power supply (#6) [31]. The elements are now explained in detail:
A typical mesh plate has a diameter of approximately 4 mm, a thickness of approximately 20 µm and contains several thousand holes. The holes in the membrane preferentially have a larger cross section at the rear side than at the front side (the side which emits the droplets). Such holes are believed to enhance dispensation of droplets (due to reduction of viscous drag). As a consequence the vibrating amplitude can be lowered. An emergent droplet usually has a 1-3 fold larger diameter than the hole diameter at the front size, which is approximately 3 µm large. Typically 10 % of the holes emit droplets [32].

The faces of the membrane do not need to be planar. „The front face may advantageously have locally raised regions immediately surrounding each hole. Such locally-raised regions are believed to enhance the dispensation of droplets by effectively pinning the menisci of the fluid adjacent to the front face of the holes. This reduces problems with droplet dispensation caused by wetting of the membrane front face by the fluid“ [32].

Figure 9 shows front view and a section (side) view of an annular mounting (piezoelectric element) holding the membrane.

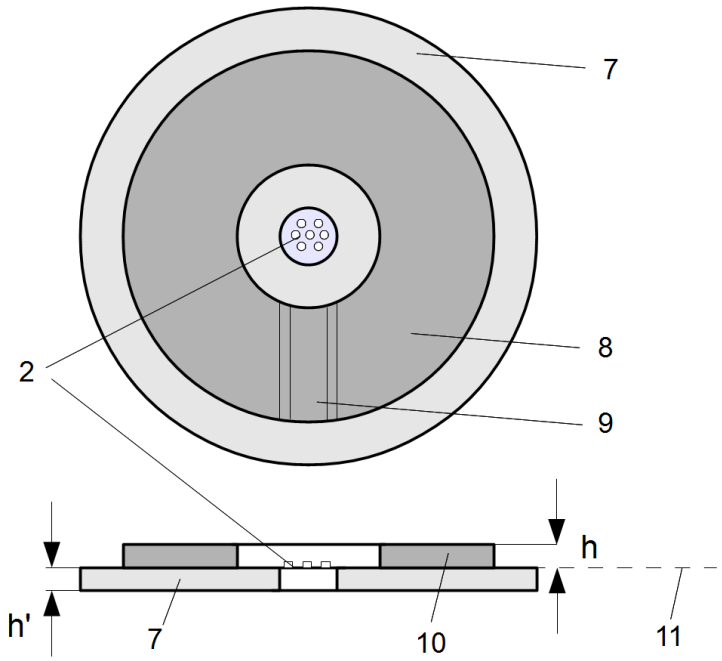

Figure 9: Schematic presentation of the annular piezoelectric disc which surrounds the membrane. Modified from [31].

The piezoelectric element consists of two layers (#7 and #10), which have a thickness of approximately 0.2 mm each and an outer diameter of 14 mm and 20 mm, respectively. The layers shorten or extend when an electric field is applied. When one layer contracts or extends bending occurs. The bilayer is asymmetrically disposed concerning the mechanical neutral axis (#11).
Either layers or just one layer (active layer) might be altered. Effective bending motion is obtained when equation 1 is satisfied [31].

$$Yh^2 \leq aY'h'^2 \tag{1}$$

Y	elastic modulus of active layer
Y′	elastic modulus of reaction layer
h	thickness of active layer
h′	thickness of reaction layer
a	dimensionless constant

If both layers are excited at the same degree, but in antiphase (180° phase shift), then bending motion is particularly effective if a lies between 0.3 and 3. Each upper surface of the two layers contains a „drive“ electrode (#7 and #8). Additionally one layer contains a „sense“ electrode (#9), which is separated from the drive electrode with a 0.5 mm air gap.

The electric equivalent circuit of the piezoelectric disc is shown in figure 10.

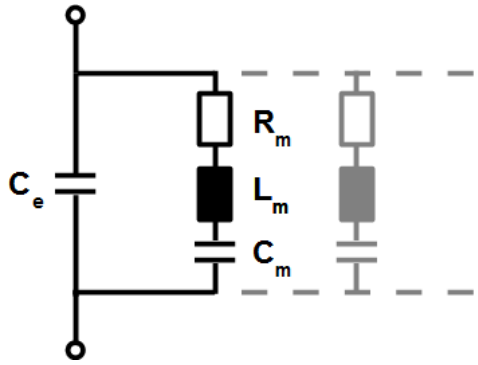

Figure 10: Electric equivalent of the actuator. Redrawn from [31].

C_e is the (static) capacity between the main electrode and the substrate electrode. The actuator exhibits several mechanically resonant frequencies, one particular frequency is represented by R_m, C_m, and L_m in the electric circuit.

The role of the electric circuit given in figure 11 is to select the one particular resonance that yields to a maximum liquid dispense. In this case this means L_m and C_m resonance. #4 is the actuator, #8 is the driving electrode, #7 is the substrate electrode connected to the ground and #9 is the sense electrode which provides a voltage signal representing motion of the actuator. Since there are several mechanically resonance frequencies for the actuator, an inductive element L_1 is added parallel to the actuator. L_1 is usually chosen, so that the resonance frequency f_r of L_1 and C_e equals the desired resonance frequency, according equation 2 [31].

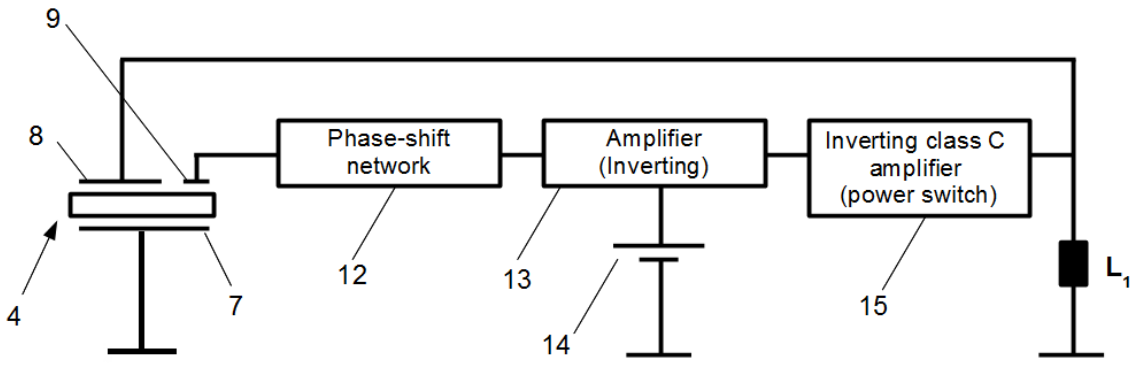

Figure 11: Block diagram of the electronics system. Redrawn from [31].

$$f_{\mathrm{r}} = \frac{1}{2\pi\sqrt{L_1 C_{\mathrm{e}}}} = \frac{1}{2\pi\sqrt{L_{\mathrm{m}} C_{\mathrm{m}}}} \tag{2}$$

The impedance of L_1 and C_{e} tends towards infinity at the resonance frequence, thus all electric power is applied directly to R_{m}, C_{m}, and L_{m}.
An inverting amplifier (#13, fig 11) provides gain at the oscillation frequency. An inverting switching element (#15) turns on and off at the drive frequency, connecting and disconnecting the actuator/L1 to a direct current power source (#14). At the resonance frequency the actuator exhibits a fast change of phase between the drive and sense electrode. A phase shift network (#12) causes a phase shift of 45° between the drive and sense electrode. The sense electrode is leading. This results in maximum fluid dispension [31].

The vibrating mesh nebulizers used in this study were the eFlow® rapid (PARI, Starnberg, Germany) and the M-neb® (Nebu-Tec, Elsenfeld, Germany).

eFlow® rapid. The eFlow® rapid operates at an oscillating frequency of 117 kHz and is protected with at least 5 US patents. Its components are shown in figure 12.

In the mixing chamber (#5a) the aerosol accumulates after generation. This aerosol bolus is inhaled in the patients inhalation phase. An exhalation valve (#7a) ensures that the exhaled air of the patient does not reach the mixing chamber. The purpose is to minimize aerosol loss during exhalation phases [34].
The aerosol production with a vibrating membrane is particularly effective, if the fluid feed takes place under a pressure slightly below the ambient pressure [35, 36]. #5 is a gas-tight fluid reservoir. When it is sealed the reservoir volume is increased mechanically,

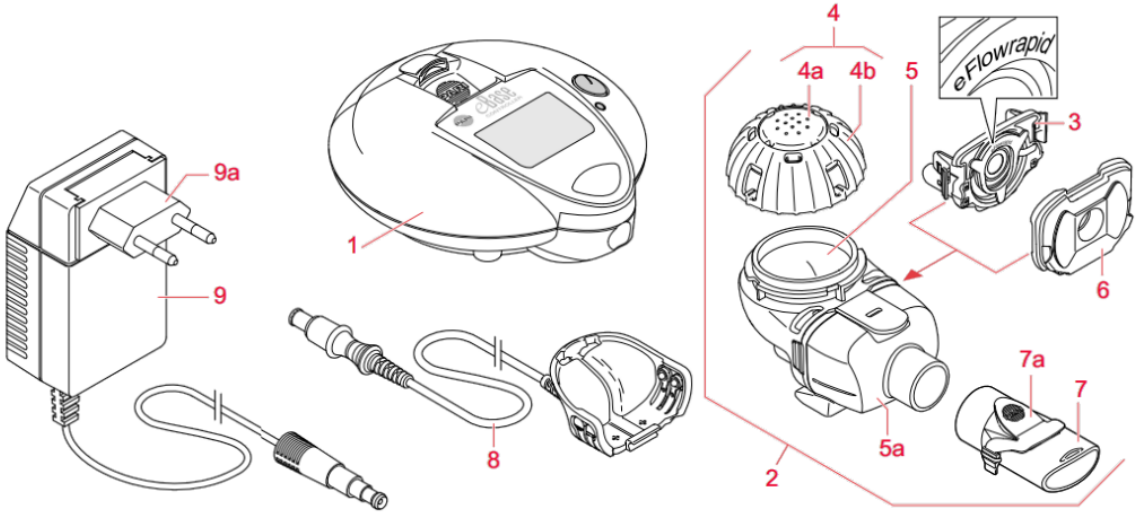

1 Control unit
2 Nebulizer handset
3 Aerosol head
4 Medication cap
4a Cap seal
4b Cap
5 Medication reservoir
5a Mixing chamber
6 Inspiratory valve
7 Mouthpiece
7a Expiratory valve
8 Connection cord (connection between control unit and nebulizer handset)
9 (International) Power adapter
9a Interchangeable adapter

Figure 12: Components of the eFlow® rapid [33].

which causes a negative pressure [36].

A problem found with all nebulizers is that a lot of aerosol is lost during exhalation phases. A mixing chamber with a one way valve was described above. Face masks and systems which adapt their nebulization rate according to the patients breathing pattern are further improvements which might be used with all nebulizer types [27, 37].

1.4 Aims of the thesis

Aim of this study was to examine different nebulizer principles on their applicability for inhalation therapy with liposomal suspensions.

For inhalation therapies liposome suspensions need to be

1. prepared
2. nebulized
3. inhaled

as shown in figure 13.

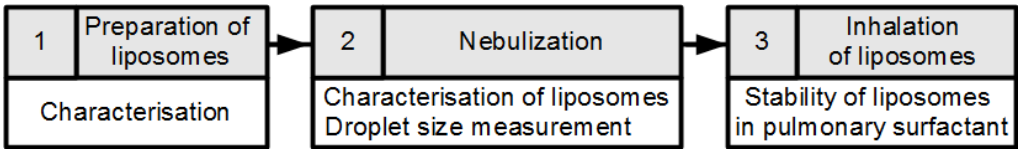

Figure 13: Inhalation therapy action steps (gray box) and measurements which were conducted in this study (white box).

The research questions and the corresponding experiments were as follows:

I: Characterization of liposomes before and after nebulization.

1. Has the nebulizer type (vibrating mesh, air-jet, ultrasonic) any influence on the stability of liposomes during nebulization?
2. Which nebulizer is most efficient for liposomal suspensions?
3. Is the transport efficacy of the M-neb® vibrating mesh nebulizer, which is under development, comparable with the efficacy of the eFlow® rapid (vibrating mesh) nebulizer?

II: Measurement of the aerosol droplet size.

1. Does the liposome surface influence the aerosol droplet size of the different nebulizers?
2. Does the salt concentration influence the aerosol droplet size of the different nebulizers?

III: Determination of ANTS/DPX leakage from liposomes in pulmonary surfactant.

1. Do the surface properties influence the stability of liposomes in pulmonary surfactant?

1.5 Structure of the thesis

Chapter 1 contains a general introduction (about liposomes and nebulizers) and the aims of this study.
Chapter 2-4 contain the three conducted experiments. Methods which stayed the same in all experiments, are being described once in chapter 2.3.
Chapter 5 contains the conclusion.

2 Nebulizer efficacy and influence on liposome stability (experiment I)

2.1 Summary

In this experiment liposomes with different surface properties were nebulized with different nebulizer types. Liposome stability depended mainly on the liposome formulation. The less liposomes were surface modified, the higher was their stability. The liposome transport efficacies were formulation independent and highest with the two vibrating mesh nebulizers (M-neb® and eFlow rapid®).

2.2 Introduction

Liposomes and nebulizers are described in chapter 1.

A commercial available liposomal inhalation solution, LipoAerosol® (Optima, Moosburg-/Wang, Germany), was nebulized additionally to the surface modified DPPC : cholesterol liposomes for comparison.
This inhalation solution consists of a physiological saline concentration ($\approx 0.8\,\%$) and phospholipid liposomes (especially phosphatidylcholin). Its purpose is to moisten the upper and lower airways and to support the natural surfactant. LipoAerosol® is sold without prescription.

2.3 Materials and methods

2.3.1 Experiment design

Each of the three formulations was nebulized with each of the three nebulizers. The whole procedure was performed three times as follows:

1. Preparation of the three different liposomal formulations. (see chapter 2.3.3)
2. Separation of liposomes from non-encapsulated fluorophore. (see chapter 2.3.4)
3. Determination of the lipid concentration (see chapter 2.3.5) and dilution to 1 mg/ml.
4. Measurement of ζ-potential (see chapter 2.3.5), liposome size (see chapter 2.3.5) and fluorescence intensity. (see chapter 2.3.5)
5. Nebulization of each of the 3 formulations with each of the 3 nebulizers. (9 nebulizations, see chapter 2.3.6)
6. Measurement of liposome size (see chapter 2.3.5), fluorescence intensity (see chapter 2.3.5) and lipid concentration (see chapter 2.3.5) in aerosol and remainder.

Nebulization studies with the M-neb® were performed twice.
Additionally to the given procedure, commercial LipoAerosol® was nebulized and characterized concerning liposome size and lipid concentration.

2.3.2 Materials

DPPC, cholesterol, DPPE–PEG_{2000}, and DOTAP were purchased from Avanti Polar Lipids (Alabaster, USA). ANTS and DPX were purchased from Sigma-Aldrich (Vienna, Austria). All other chemicals were purchased from Carl Roth (Karlsruhe, Germany).
The applied nebulizers were the MicroDrop MasterJet® air-jet nebulizer (MPV Truma, Putzbrunn, Germany), the Optineb®-ir ultrasonic nebulizer (Nebu-Tec, Elsenfeld, Germany), the eFlow® rapid vibrating mesh nebulizer (Pari, Starnberg, Germany), and the M-neb® vibrating mesh nebulizer (Nebu-Tec, Elsenfeld, Germany).

2.3.3 Preparation of liposomes

Liposomes were prepared according to the lipid hydration method [1]:

1. Lipid composition:
   The stock solutions were prepared in chloroform : methanol (2:1, v/v). From these stock solutions the three formulations given in table 1 were prepared, with a total lipid mass of 18.4 mg/ml. The concentration of cholesterol is 3.4 mg/ml for all three formulations.

Table 1: The three liposomal formulations and their lipid composition (χ is the mole fraction).

Formulation	DPPC χ in %	cholesterol χ in %	DPPE–PEG_{2000} χ in %	DOTAP χ in %
F1	70	30	-	-
F2	66.2	31.8	2	-
F3	59.3	31.7	2	7

   The lipid mixtures were vortexed and the organic solvent was evaporated under a stream of nitrogen. Probes were completely dried in a vacuum chamber overnight.

2. Rehydration
   Each dry film was rehydrated with 1 ml buffer (pH 7.4), which was prepared according to table 2.

Table 2: Components of the rehydration buffer.

	HEPES[4] mM	NaCl mM	ANTS mM	DPX mM
Rehydration buffer I	10	68	12.5	45
Rehydration buffer II (no ANTS/DPX)	10	140	-	-

The rehydration buffer II was used when no ANTS/DPX leakage assay was performed (experiment II). Formulations were incubated at 52 °C for 2 hours and vortexed every 15 minutes for 1 minute. 52 °C were chosen because 41 °C is the phase transition temperature of DPPC and Kleemann et al (2007) determined a phase transition temperature of 53 °C for DPPC : cholesterol [38]. The probes were protected from light, in order to avoid photobleaching of the fluorophore.

3. Extrusion
   Probes were extruded with a mini extruder (Avanti Polar lipids, USA), which was heated to 52 °C. The polycarbonate membrane had a pore size of 100 nm (Whatman, Dassel, Germany) and probe was pressed through it 41 times. Afterwards a size-check was performed (see chapter 2.3.5). If liposomes were larger than 200 nm or polydispersity index was higher than 0.2, extrusion was repeated.

   For extended storage, liposomes were stored at 4 °C, protected from light.

2.3.4 Separation of liposomes from non-encapsulated fluorophore

Liposomes were separated from non-encapsulated fluorophore with gel filtration chromatography (size exclusion).

1. Preparation of the column
   Plastic columns with a height of 14 cm and a width of 1.5 cm (Econo-PacR 10DG Desalting Columns, Bio-Rad Laboratories, Hercules, USA) were emptied and filled with soaked Sephadex G-75. A small portion of sodium azide was added to prevent bacterial growth. Two frits (membranes) were used to enclose the soaked Sephadex. A 10 mM HEPES buffer with 140 mM NaCl (pH 7.4) was used for swelling the gel and purification of liposomes.

2. Purification
   First the column was washed twice with elution buffer (the HEPES buffer mentioned above). When the buffer reached the upper frit, 1 ml probe was pipetted into the

column. Short time afterwards, when the probe reached the upper frit, buffer was filled into the column. Drops were collected in 1.5 ml microcentrifuge tubes (Eppendorf, Hamburg, Germany) at the bottom of the column. The turbid, liposomes containing fractions were visually determined and pooled.

2.3.5 Measurements (Size, concentration, fluorescence, ζ-potential)

Size measurement of liposomes. Size measurement was performed via dynamic light scattering (DLS) with a zetasizer 3000HSA (Malvern Instruments, Herrenberg, Germany). The 10 mW helium-neon laser operated at a wavelength of 632.8 nm. The temperature was 25 °C. The result consists of two values. The Z-Average, which is the intensity weighted mean hydrodynamic diameter, and the polydispersity index (PDI), which is a dimensionless measure of the broadness of the size distribution. The PDI ranges from 0 (monodispers) to 1 (polydispers). For the measurement samples were diluted to a lipid concentration of approximately 1 µg/ml with bidistillated, filtrated (0.02 µm filter, Whatman, Dassel, Germany) water.

Lipid concentration determination. The lipid concentration was calculated from the phosphatidylcholine (PC) concentration, according to the molar ratios of each formulation. The PC content was determined with the enzymatic colorimetric Phospholipide FS™ set from DiaSys (Holzheim, Germany) [39]. The principle is as follows:
Two reagents (reagent 1: TRIS[5] buffer (pH 8.0), TBHBA[6], choline oxidase, detergents and stabilizers; reagent 2: TRIS buffer (pH 8.0), 4-Aminoantipyrine, peroxidase, phospholipase D, detergents, stabilizers and preservatives) are added to the samples. Those reagents generate a chinone dye, depending on the PC concentration [39]:

$$\begin{aligned} \text{phosphatidylcholine} + H_2O &\xrightarrow{\text{phospholipaseD}} \text{choline} + \text{phosphatidic acid} \\ \text{choline} + 2\,O_2 + H_2O &\xrightarrow{\text{choline oxidase}} \text{betaine} + 2\,H_2O_2 \\ 2\,H_2O_2 + \text{4-aminoantipyrine} + \text{TBHBA} &\xrightarrow{\text{peroxidase}} \text{chinone dye} + 4\,H_2O \end{aligned}$$

The absorbance of the dye in the samples and in a phospholipid standard was measured with a Hitachi U2000 spectrophotometer (Hitachi High-Technologies, Krefeld, Germany) at a wavelength of 570 nm. The detailed procedure was as follows:

- addition of reagent 1 to the samples
- incubation of the samples at 37° C for 5 minutes
- measurement of absorbance 1

[5] tris(hydroxymethyl)aminomethane
[6] 2,4,6-tribromo-3-hydroxybenzoic acid

- addition of reagent 2
- incubation at 37° C for 5 minutes
- measurement of absorbance 2

Each measurement was done in duplicates. The corresponding equations can be found in section 2.3.7.

Fluorescence intensity measurement. Fluorescence was measured with a SPEX FLUOROMAX-3 (HORIBA Jobin-Yvon, Unterhaching, Germany), which has a Xenon arc lamp as a light source. All measurements were conducted at 37 °C and with a slit size of 5 nm for both filters. The time settings for the spectra measurements (of ANTS/DPX) and the fluorescence intensity measurements can be seen in table 3.

Table 3: Time settings for fluorescence measurements in experiment I.

	without Triton X-100™			after addition of Triton X-100™		
	$t_{integration}$ s	$t_{repetition}$ s	t_{total} s	$t_{integration}$ s	$t_{repetition}$ s	t_{total} s
Spectra measurements	0.1	-	-	-	-	-
Fluorescence intensity	0.1	2	160	0.1	2	160

An 101-QS 10 x 10 mm quartz cuvette (Hellma Analytics, Müllheim, Germany) was used in the measurements. Samples (25 µl) were diluted in 2 ml HEPES buffer (10 mM HEPES, 140 mM NaCl, pH 7.4).

The excitation spectrum of ANTS/DPX was measured with a fixed emission wavelength filter of 530 nm. The excitation wavelength filter was altered from 250 to 460 nm in 1 nm steps.
The emission spectrum was measured with a fixed excitation wavelength filter of 360 nm and the excitation wavelength filter was altered from 400 to 650 nm. The concentrations of ANTS and DPX in the spectra measurements before dilution were the same as in the remaining experiment I.

In experiment I excitation wavelength filter was set to 360 nm, emission filter to 530 nm. Measurements were repeated after the addition of 10 µl 10% Triton X-100™ . Each sample was measured at least twice.

ζ-potential measurement (of liposomes). The ζ-potential was measured with a zetasizer NanoZS/ZEN3600 (Malvern Instruments, Herrenberg, Germany), which combines an electrophoresis and a laser doppler velocimetry. Measurement was conducted with a folded capillary cell (Malvern Instruments).
Liposomes were prepared without NaCl for the ζ-potential measurement. NaCl free columns were used for the separation of liposomes from non-encapsulated fluorophore. Probes were diluted to a final lipid concentration of 0.3 mg/ml with 2 mM CsCl and 2 mM HEPES.

2.3.6 Nebulization set up

The idea was to collect the nebulized aerosol droplets in a 50 ml falcon tube (Greiner Bio One, Kremsmünster, Österreich), which is being cooled to 4 °C by a condensate collecting system (TURBO-DECCS, Parma, Italy). The falcon tube and the nebulizer were connected with a 30 cm long plastic pipe. Since the nebulizers have different airflow rates, a compressor (DeVO/MC 29, DeVilbiss Healthcare, Mannheim, Germany) to enhance airflow (for low flow rate Optineb®-ir) or an additional collecting vessel (for high flow rate MicroDrop MasterJet®) were applied. Figure 14 shows the set up for the different nebulizers.

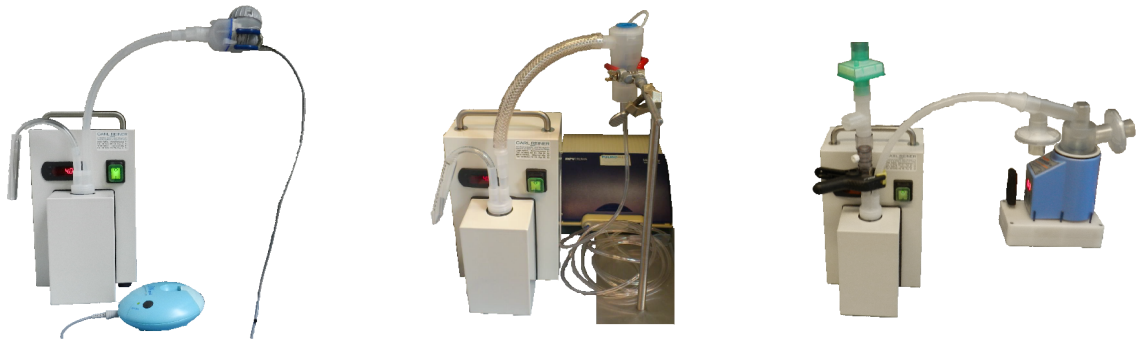

(a) eFlow® rapid (b) MicroDrop MasterJet® (c) Optineb®-ir

Figure 14: The nebulization set up for the nebulizers. Power supply and compressor for the Optineb®-ir are not shown.

Each nebulizer reservoir was filled with 3 ml of liposomal suspension and 2 ml thereof were nebulized. Therefore the nebulizers were weighed before and after nebulization. The fluid that is retained in the reservoir within the nebulizer is referred to as the „remainder“.

2.3.7 Equations and calculations

The mass of each lipid for each formulation was calculated with equation 3 and the help of the mole fractions in table 1.

$$m_{\text{lipid}} = \underbrace{\frac{\chi_{\text{lipid}} \cdot M_{\text{lipid}}}{\sum\limits_{\text{n=lipids}} \chi_{\text{n}} \cdot M_{\text{n}}}}_{w_{\text{lipid}}} \cdot m_{\text{total}} \tag{3}$$

m_{total}	mass of all lipids together (18.4 mg)
M	molar mass
w_{lipid}	mass fraction of the lipid
χ	mole fraction

The PC concentration in the Phospholipide FS™ test was calculated according to the manual [39]:

$$c_{\text{phospholipids}} \left[\frac{mg}{ml}\right] = \frac{\Delta A_{\text{sample}}}{\Delta A_{\text{standard}}} \cdot c_{\text{standard}} \tag{4}$$

c_{standard}	PC concentration of the standard. (3.1 mg/ml)
ΔA_{sample}	Difference of second (A2) and first (A1) absorbance measurement. ($A2_{\text{sample}}$ - $A1_{\text{sample}}$)
$\Delta A_{\text{standard}}$	$A2_{\text{standard}}$ - $A1_{\text{standard}}$. Since simultaneous absorbance measurements were not possible, the absorbance of the standard was measured before and after the samples. The values for A1 and A2 were obtained by linear interpolation of the original measured values.

The total lipid concentration was calculated from the PC concentration, according to the molar ratios of the formulations given in table 1.

$$c_{\text{total}} = \underbrace{\frac{c_{\text{DPPC}}}{M_{\text{DPPC}} \cdot \chi_{\text{DPPC}}}}_{c_{\text{i\_total}}} \cdot \underbrace{\sum_{\text{n=lipids}} M_{\text{n}} \cdot \chi_{\text{n}}}_{M_{\text{total}}} \tag{5}$$

χ_{DPPC}	mole fraction of DPPC.
c_{DPPC}	DPPC concentration.
$c_{\text{i\_total}}$	total molar concentration.
c_{total}	total lipid concentration.
M_{DPPC}	molar mass of DPPC.
M_{total}	total molar mass.

Note: The mass fraction of cholesterol is the same for all formulations. Thus the mentioned 1 mg/ml lipid concentration in this thesis is the value for all lipids except cholesterol. The total lipid concentration including cholesterol was actually 1.24 mg/ml.

The relative lipid concentration in aerosol and remainder was calculated by dividing the concentration with the initial (start) concentration according to equation (6).

$$c\ [\%] = \frac{c_\mathrm{t}}{c_\mathrm{s}} \cdot 100 \tag{6}$$

c_t	lipid concentration in aerosol or remainder.
c_s	lipid concentration at the start.

Encapsulation is the ratio of the fluorescence intensity increase due to the addition of Triton X-100™to the overall fluorescence intensity after addition of Triton X-100™:

$$\mathit{encapsulation}\ [\%] = \frac{I_\mathrm{T} - I_\mathrm{t}}{I_\mathrm{T}} \cdot 100 \tag{7}$$

I_t	fluorescence intensity of probe before the addition of Triton X-100™.
I_T	fluorescence intensity after the addition of Triton X-100™.

The total fluorescence intensity in fig 16 is the fluorescence intensity (of aerosol or remainder) after the addition of Triton X-100™ divided by the fluorescence intensity before nebulization (with Triton X-100™):

$$I_\mathrm{total}\ [\%] = \frac{I_\mathrm{T}}{I_\mathrm{S}} \cdot 100 \tag{8}$$

I_S	fluorescence intensity of the sample at the start (before nebulization) after the addition of Triton X-100™.

The leakage is usually calculated according to equation (9). This equation is widely used in ANTS/DPX leakage assays [7, 8, 13, 14].

$$\mathit{leakage}\ [\%] = \frac{I_\mathrm{t} - I_\mathrm{s}}{I_\mathrm{S} - I_\mathrm{s}} \cdot 100 \tag{9}$$

I_s	fluorescence intensity of the sample at the start (before nebulization), without Triton X-100™.

Equation 9 is applied when the concentration does not change. In the case of nebulization,

concentrations of liposomes and fluorophore do change. This is why the author introduced the correction factor (I_S/I_T). The modified equation (10) is as follows:

$$leakage\ [\%] = \frac{I_t \cdot \left(\frac{I_S}{I_T}\right) - I_s}{I_S - I_s} \cdot 100 \tag{10}$$

2.3.8 Statistical analysis

Experiments were carried out three times. If not, the number (n) of experiments is stated. In the tables values are presented as mean ± standard deviation (SD). In the bar charts the error bars show minimum and maximum values. An Analysis of Variance (ANOVA) or a student's t-test was performed to determine statistically significant differences between the means of two or more groups. Differences were considered as significant if their statistical probability was higher than 95 % ($\alpha = 0.05$).

An **one-way ANOVA** was applied before nebulization for analysis of size, PDI, and encapsulation (parameter = formulation).
The **two-way ANOVA** with repetition was applied after nebulization for PDI, size change, concentration, leakage and total fluorescence intensity (parameters = formulation, nebulizer).

A **pairwise t-test** was applied to size (pair: before and after purification), once again to size (pair: before nebulization and after nebulization), and leakage analysis (pair: aerosol and remainder).

If the one-way ANOVA showed differences between the groups, 3 student's **t-tests with same variances** were used to compare the three groups with each other. A Bonferroni correction was made ($\alpha' = \alpha/3$) and a group was considered to be either bigger or smaller if the one tailed p-value (p') was below α'. The same was done for the two-way ANOVA: If there were differences, groups were pooled regarding the concerning parameter and compared to each other. For example if the two-way ANOVA resulted in a p-value below α concerning the nebulizers, then the three formulations which were nebulized with the same nebulizer were pooled and compared with the pooled formulations nebulized by the other nebulizers.

Furthermore the Pearson correlation coefficient was determined between PDI and leakage. Results of the M-neb® in the first experiment (n<3) were not analyzed.

2.4 Results

2.4.1 Characterization of liposomes before nebulization

In the spectra measurements the peak excitation of ANTS/DPX could be detected at 359 nm, the peak emission at 515 nm.

The characteristics of the liposomal formulations before nebulization are shown in table 4.

Table 4: Liposome characteristics before nebulization.

	hydrodynamic diameter nm	PDI 1	ζ-potential mV	encapsulation efficiency %
F1	165 ± 5	0.05 ± 0.01	−36.2 ± 1.1	74 ± 4
F2	140 ± 8	0.06 ± 0.02	− 0.3	84 ± 1
F3	142 ± 6	0.07 ± 0.04	14.8 ± 0.7	73 ± 2

Size. After preparation F1 liposomes were larger than F2 ($p<0.001<\alpha'$, n=4) and F3 ($p<0.001<\alpha'$, n=4) liposomes, even though all liposomes were extruded through a 100 nm filter.
Purification with the column had no significant influence ($p=0.28>\alpha$, n=9) on the size.
The liposomes from commercial LipoAerosol® had a hydrodynamic diameter of 91.5 nm.

PDI. After preparation there was no significant difference between the formulations concerning the PDI ($p=0.76>\alpha$). All liposomes were highly monodispers.

ζ-potential. The third liposomal formulation, which contains the cationic lipid DOTAP, had a positive ζ-potential. Two measurements concerning F2 had to be excluded, because a very small peak was detected at the lower end of the measurement scale. This peak distorted the result completely. The huge peak around 0 mV which appeared in all the F2 measurements was considered to be correct.

Encapsulation. F2 liposomes had the highest encapsulation after preparation, 84 ± 1 %. The difference was not significant compared to F1 liposomes ($p=0.022>\alpha'$, n=4) but significant compared to F3 liposomes ($p=0.005 <=\alpha'$, n=4).

2.4.2 Nebulizer transport efficacy

Output. Nebulization time and output were similar for all liposomal formulations and are shown in table 5.

Table 5: Nebulization time and liquid output of the nebulizers. (n=3)

	nebulization time min	output mg	output per time $mg \cdot min^{-1}$
eFlow® rapid	3.0 ± 0.3	700 ± 60	230 ± 20
MicroDrop MasterJet®	9.5	1500 ± 80	160 ± 10
Optineb®-ir	20.0	1600 ± 100	80 ± 10

The difference between the output of liposomal suspension at the mouthpiece (emitted dose) and the nebulized 2 ml, condensed at the walls inside the nebulizer. 300-500 µl of the aerosol which left the mouthpiece could be collected within the condensation chamber (delivered dose). The rest condensed at the connecting pipe or vanished into the air. In the eFlow® rapid approximately 1 ml condensed in the mixing chamber between mesh and mouth piece.
Concerning both, nebulization time and output per minute of liposomal suspensions, the eFlow® rapid nebulizer is the most effective one, the Optineb®-ir the least.

Lipid concentration. Figure 15 shows that the Optineb®-ir was the least efficient nebulizer concerning liposome transport.

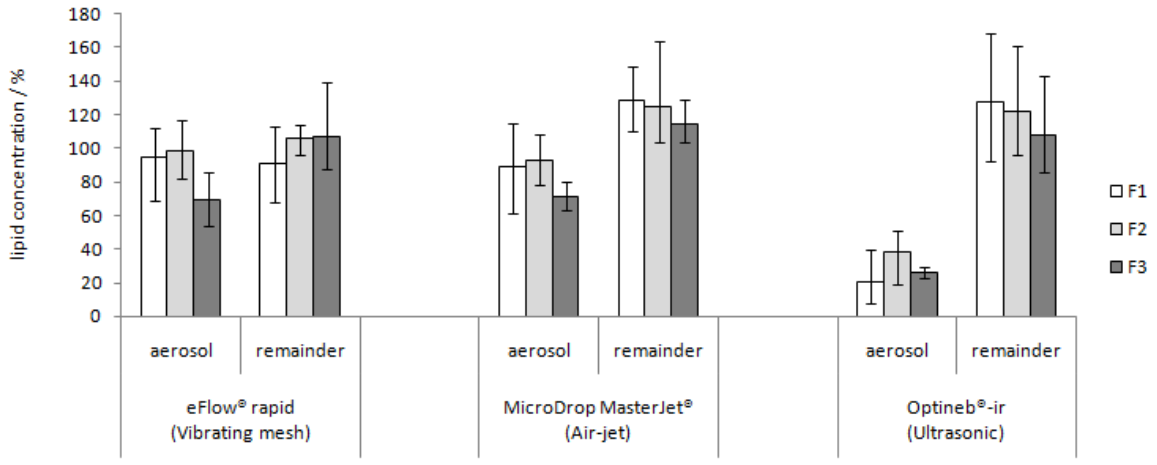

Figure 15: Mean concentration of lipids in aerosol and remainder. (% of start concentration, n=3, error bars show min/max.)

Aerosol: The concentration of lipids in the aerosol from the Optineb®-ir was very low compared to the eFlow® rapid ($p'<0.001<\alpha'$) and the MicroDrop MasterJet® ($p'<0.001<\alpha'$). There was no significant difference between the formulations ($p\approx0.05>\alpha$).
Remainder: There were neither differences concerning formulations ($p=0.76>\alpha$) nor nebulizers ($p=0.26>\alpha$).

Total fluorescence intensity. The total fluorescence intensity is the fluorescence intensity after addition of Triton X-100™. Since most of the fluorophore is still encapsulated after nebulization, the total fluorescence intensity is linked to the lipid concentration. Fluorescence intensity was lowest in the aerosol of the Optineb®-ir, as shown in figure 16.

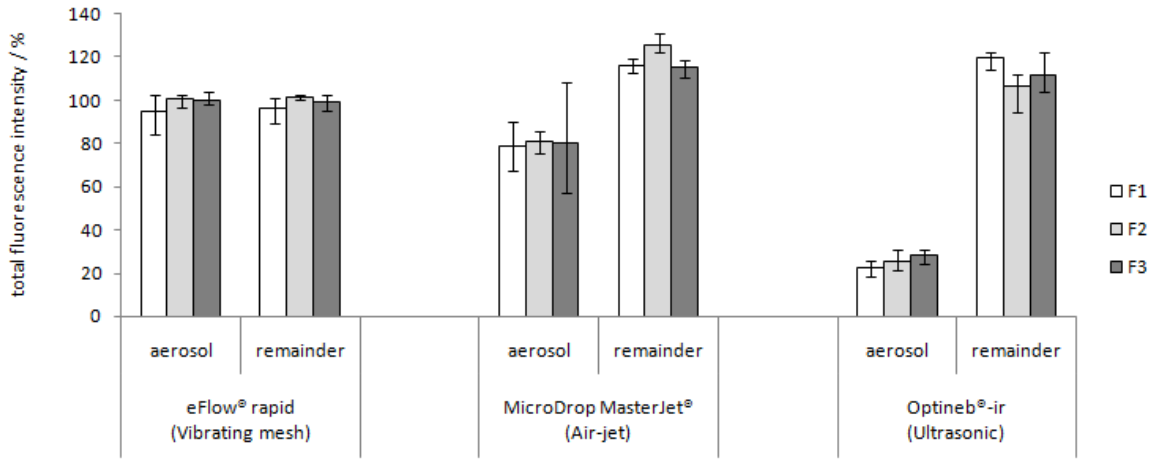

Figure 16: Mean fluorescence intensity after addition of Triton X-100™, relative to start value; n=3, error bars show min/max.

Aerosol: In the aerosol of the eFlow® rapid, a higher fluorescence intensity than in the aerosol of the MicroDrop MasterJet® could be detected. Furthermore aerosol of those two nebulizers exhibited a higher fluorescence intensity than the aerosol of the Optineb®-ir ($p'<0.001<\alpha'$ for all 3 comparisons).
Remainder: A lower fluorescence intensity was detected in the remainder of the eFlow® rapid compared to the MicroDrop MasterJet® and the Optineb®-ir ($p'<0.001<\alpha'$ for both comparisons).

LipoAerosol®. The PC concentrations of LipoAerosol® in aerosol and remainder after nebulization are shown in table 6. A comparison with fig 15 shows, that the liposomal transport efficiency depends on the nebulizer device, not the liposomal formulation.

Table 6: PC concentration of LipoAerosol® in aerosol and remainder, n=1. (% of start concentration)

	aerosol c in %	remainder c in %
eFlow® rapid	111	102
MicroDrop MasterJet®	75	108
Optineb®-ir	32	101

The initial PC concentration was measured as 8.2 mg/ml and should be 10 mg/ml, according to the description.

2.4.3 Nebulization: Stability of liposomes

Size change. The size of liposomes after nebulization was compared with the size before nebulization and marked with an asterisk (*) if there was a significant difference. Figure 17 shows the size change. In general, changes in size were minor.

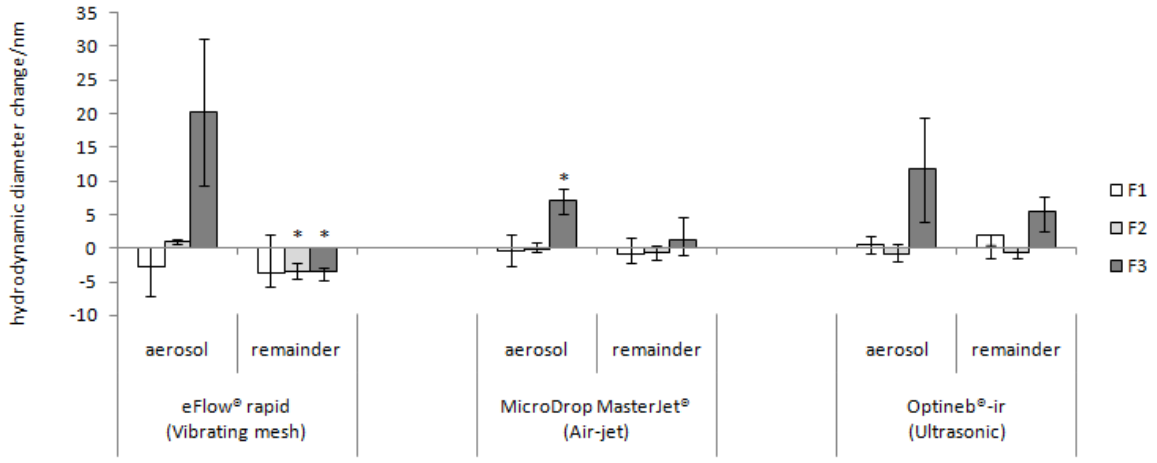

Figure 17: Mean size change of liposomes due to nebulization; n=3, error bars show min/max.

Aerosol: F3 Liposomes became larger (p=0.022<α for all) after nebulization with the MicroDrop MasterJet®. F3 liposomes had a larger size increase than F2 and F1 liposomes (p<0.001<α for both).
Remainder: F2 (p=0.041<α) and F3 (p=0.028<α) liposomes became smaller during nebulization with the eFlow® rapid. In general liposomes nebulized with the vibrating mesh nebulizer showed the biggest decrease in size in the remainder, compared with the air-jet

(p=0.001<α') and the ultrasonic nebulizer (p= 0.001<α').

Liposomes of LipoAerosol® increased by 0.3 nm, when nebulized with the eFlow® rapid (n=1).

PDI. The surface modified liposomes had a wider size distribution after nebulization, as shown in figure 18.

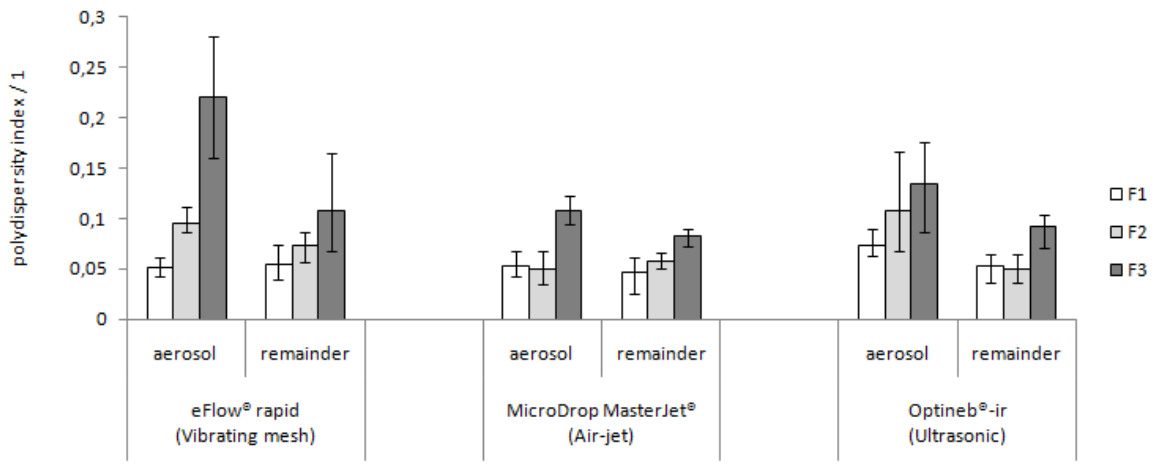

Figure 18: Mean PDI of liposomes after nebulization; n=3, error bars show min/max.

Aerosol: F3 liposomes had a wider size distribution than F1 (p=0.001<α') and F2 (p=0.012<α') liposomes. There was interaction (p=0.028<α) between formulation and nebulizer, which means that special combinations (for example eFlow® rapid and F3) have a huge impact on the PDI.
Remainder: F3 liposomes had a higher polydispersity than F1 (p=0.001<α') and F2 (p=0.008<α') liposomes, like in the aerosol.

The correlation coefficient between leakage and PDI in the aerosol is 0.90 (n=33, all 4 nebulizers). If one outlier is excluded, the coefficient is even 0.94. The similarity between leakage and PDI can be seen in fig 18 and fig 19. The correlation coefficient for leakage and PDI in the remainder is 0.80.

Leakage. The leakage of ANTS/DPX was lowest with the unmodified F1 liposomes, as shown in figure 19.

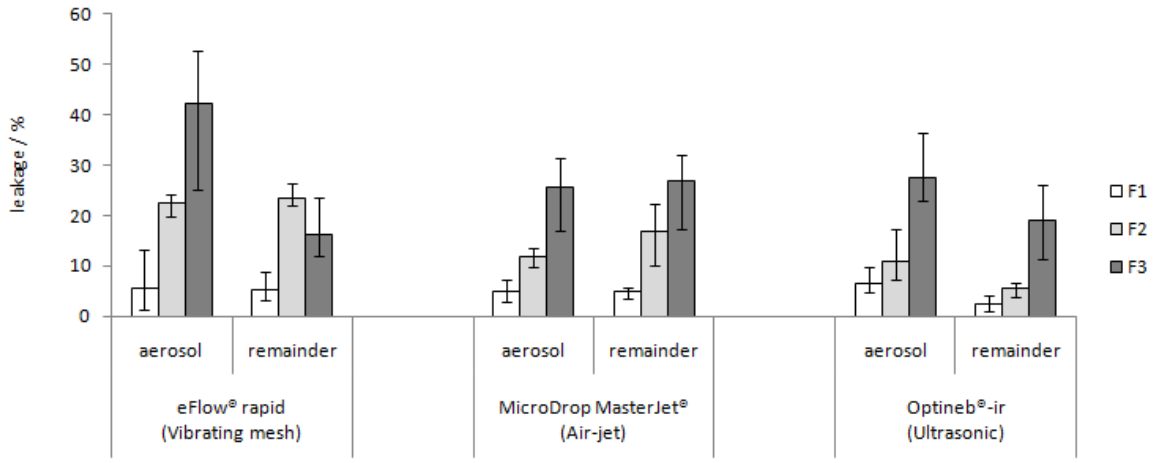

Figure 19: Mean leakage of the initially encapsulated fluorophore; n=3 error bars show min/max.

Aerosol: The highest leakage was seen with F3, the smallest with F1 liposomes. The difference between the formulations was significant ($p<0.002<\alpha'$ for all three comparisons).
Remainder: Leakage from F1 liposomes was smaller than leakage from F2 and F3 liposomes ($p<0.002<\alpha'$ for both comparisons).
A pairwise comparison of aerosol and remainder revealed, that leakage was larger in the aerosol than in the remainder of the Optineb®-ir ($p=0.003<\alpha$).

2.4.4 Comparison of the two vibrating mesh nebulizers

The results of the eFlow® rapid in this chapter (n=3) are the same as in the previous chapter. They were reprinted in this chapter to enable direct comparison with the M-neb® (n=2).

Nebulization time and output It took the M-neb® approximately 10 minutes to nebulize 2 ml of the liposomal suspensions. The nebulization time fell to approximately 6 minutes, when the nebulization set up was changed and the aerosol was collected straightforward with the condensate collecting system without any plastic pipe in between. The output was approximately 1800 mg.

Lipid concentration. Both vibrating mesh nebulizers showed a high efficacy to transport liposomes, as presented in figure 20.

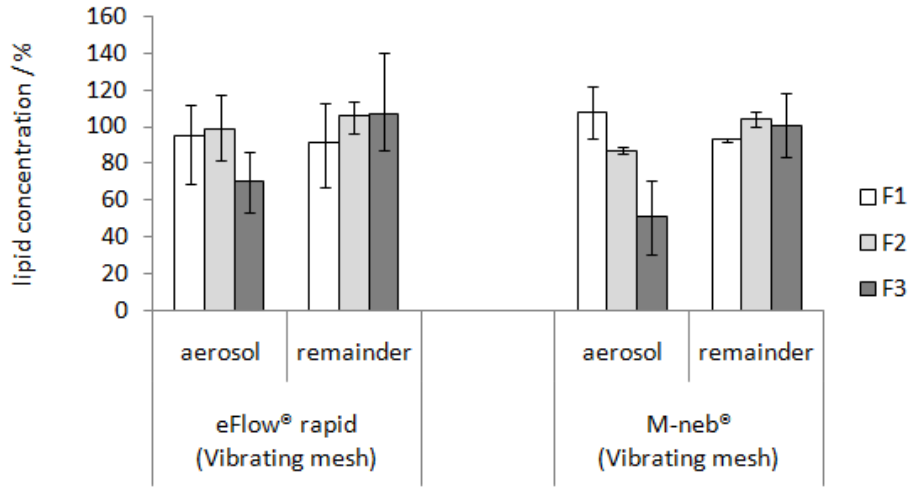

Figure 20: Mean concentration of lipids in aerosol and remainder, after nebulization with the eFlow® rapid (n=3) and the M-neb® (n=2). (% of start concentration; error bars show min/max.)

Total fluorescence intensity. The total fluorescence intensity, which is linked to to liposomal transport, shows that the M-neb® is very efficient, as shown in figure 21.

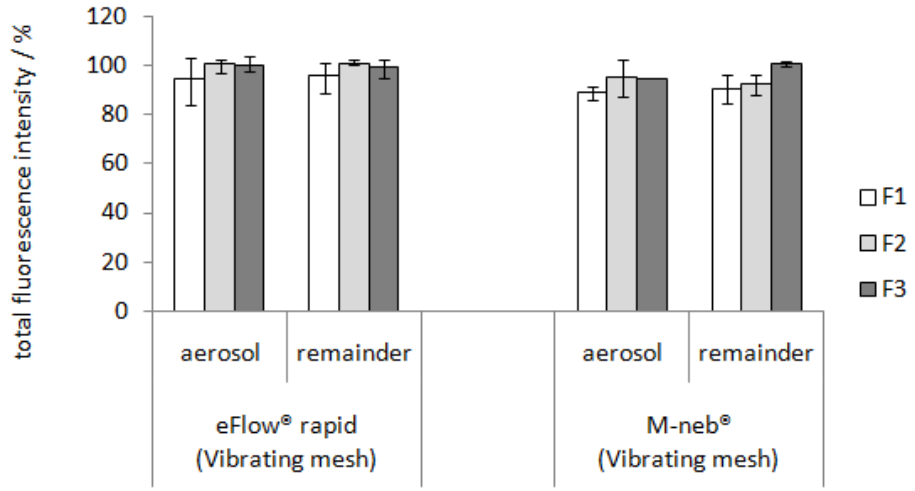

Figure 21: Mean total fluorescence intensity, compared to the initiall intensity. (n=3 for eFlow® rapid and n=2 for M-neb®; error bars show min/max.)

Size change. In the aerosol, F3 liposomes nebulized with the M-neb® showed a big increase in size, as shown in figure 22.

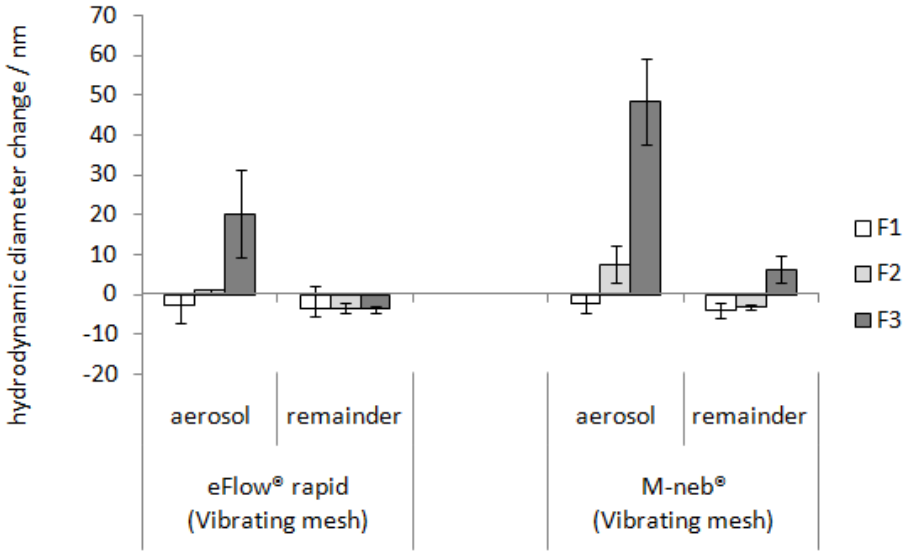

Figure 22: Mean size change (n=3 for eFlow® rapid and n=2 for M-neb®; error bars show min/max.)

Leakage. Leakage from liposomes was approximately the same for both vibrating mesh nebulizers, as shown in figure 23.

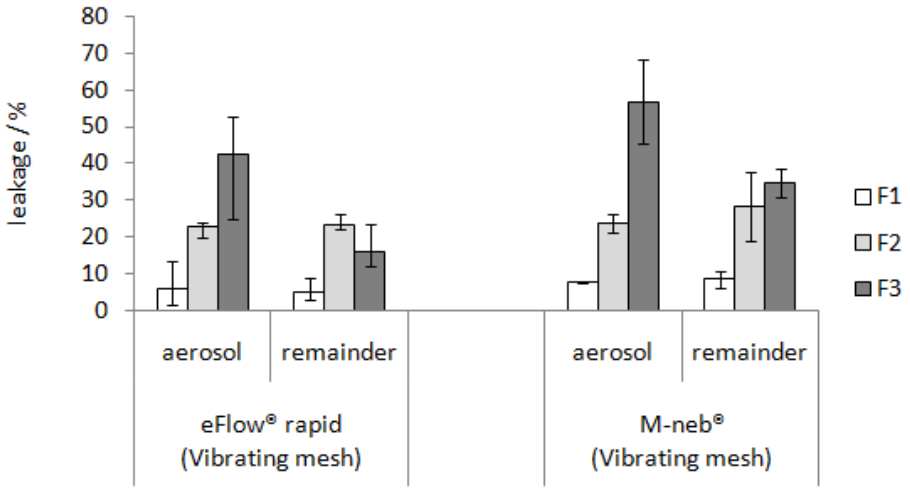

Figure 23: Mean leakage of initially encapsulated fluorophore (n=3 for eFlow® rapid and n=2 for M-neb®; error bars show min/max.)

2.5 Discussion

2.5.1 Characterization of liposomes before nebulization

Spectra. In the spectra measurements the ANTS/DPX concentrations as in experiment I were used. The concentration was not altered in order to avoid artifacts which might appear due to high concentrations. However the concentration was too low to get a satisfactory signal to noise ratio. Thus the slit size was increased from 1 to 5 nm, the same slit size which was used in the other measurements. This caused smoothing and may slightly shift the peak wavelengths. Spectra were lamp corrected. The background fluorescence intensity from the buffer was not subtracted due to a poor signal to noise ratio. In all further measurements excitation and emission wavelengths were set to 360 and 530 nm, respectively. Emission wavelength filters with 530 nm are widely used in ANTS/DPX experiments [7–10]. Further literature research revealed, that there are several studies with an emission wavelength filter set to 520 nm [11–15].

Size. The particle size is given in terms of the hydrodynamic diameter which was measured with dynamic light scattering. The hydrodynamic diameter depends on the translational diffusion coefficient. It is the way a particle diffuses within a fluid. The translational diffusion coefficient of the particle depends on the core, the lipid concentration, and type of ions in the medium. The hydrodynamic diameter might differ from the „core“ diameter, as shown in figure 24. This might be the reason, why all formulations were larger

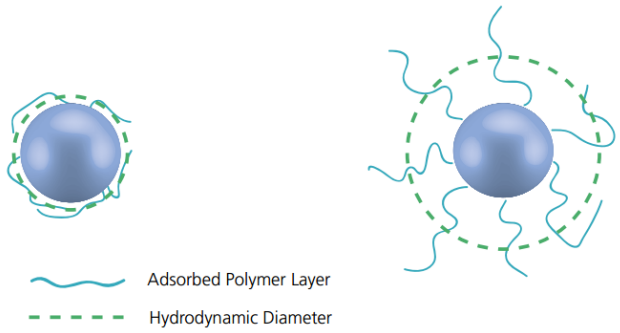

Figure 24: The hydrodynamic diameter

than 100 nm after an extrusion through a 100 nm filter. The second explanation is, that liposomes might not be spherical, but elongated.

Opposed to the explanation with the hydrodynamic diameter is the finding that the incorporation of DPPE–PEG decreased size of liposome, as shown before in table 4. This

finding is confirmed by a previous study:
Kleemann et al (2007) showed that the incorporation of DPPE–PEG reduces size of DPPC : cholesterol liposomes. After extrusion through a 400 nm filter, liposomes had diameters of approximately 400 (without DPPE–PEG) and 250 nm (with DPPE–PEG) [38].
Furthermore Cinelli et al (2007) showed that the incorporation of DOTAP decreases size of DPPC structures in aqueous solutions [40].

Encapsulation. The calculated encapsulation at the start, after removal of the non-encapsulated fluorophore with chromatography column, was not 100 % as one could assume. The fluorescence which could be detected without addition of Triton X-100™ was on one hand from the background (lipids and buffer). This accounted for approximately one third of the fluorescence. On the other hand fluorescence probably came from fluorophore which was attached to the outer side of the liposomes or the PEGylation. The second formulation, F2, showed a higher encapsulation than the other two formulations. This might be due to the neutral ζ-potential. The potential of F1 and F3 liposomes might influence polyanionic ANTS and cationic DPX.

2.5.2 Nebulizer transport efficacy

The MicroDrop MasterJet® was always turned on for 9:30 minutes and the Optineb®-ir was always activated 30 times, and thus both ran always for the same time. The eFlow® rapid was the only nebulizer which had varying nebulization times, because it stops automatically when just 1 ml is left inside. The output rates were similar for all formulations. The vibrating mesh nebulizers were the most efficient nebulizers.

The nebulization set up causes a high air resistance. At least for the eFlow® rapid and the MicroDrop MasterJet®. The air resistance might be the reason, why the output rates in the experiment were lower than specified in the corresponding manuals. (Manuals: 500 mg/ml for the eFlow® rapid, >400 mg/ml for the MicroDrop MasterJet®, and 500 mg/ml for the Optineb®-ir.) When a patient inhales, probably hardly any condensate is collected inside the eFlow® rapids mixing chamber. When the codensate inside the mixing chamber is considered as output, then the output rate of the eFlow® rapid is 570 mg/ml.

The ultrasonic nebulizer, the Optineb®-ir, was unable to transport liposomes efficiently. The lipid concentration was very small in the aerosol produced by the ultrasonic nebulizer. In the remainder, concentration was slightly higher, compared to the start concentration.

We assume that the missing difference might be stuck to the walls inside the nebulizer and the connecting tube (approximately 1 mg lipids).
In contrast, the vibrating mesh nebulizers transported almost all liposomes.

The lipid concentration measurement with the Phospholipids FS™ set resulted in high standard deviations. However, it can be excluded that the concentration of ANTS/DPX influenced the result, because ANTS/DPX is not excited at 570 nm. A probe with solely ANTS/DPX yielded a lipid concentration of zero.

The fluorescence intensity after addition of Triton X-100™ is a measure for the overall amount of fluorophore in the sample. Since most fluorophore is enclosed in the liposomes, the total fluorescence intensity might be a better indicator for liposome transport than the concentration determination with the Phospholipids FS™ set, because the total fluorescence intensity measurements had smaller standard deviations than the concentration determinations (see fig 15 and fig 16).

2.5.3 Nebulization: Stability of liposomes

The surface modifications (incorporation of DPPE–PEG_{2000} and DOTAP) decreased the stability of the liposomes.
In a simulation study Tieleman et al (2002) showed that DPPC bilayers are stable up to a lateral pressure of $-2 \cdot 10^7\,\mathrm{N/m^2}$ or an electric field of $0.5\,\mathrm{V/nm}$ [41].

PDI. The PDI after nebulization correlated highly with the leakage, in particular in the aerosol. Correlation was higher for the absolute PDI than the PDI change. The PDI is easier to determine than the leakage, because no fluorophore is needed, no column chromatography and no fluorescence measurement. This method (just determining the PDI instead of the leakage) is probably a fast and good estimate for the stability of new formulations.

Leakage. There are several explanations, why aerosol and remainder might differ concerning leakage. At the beginning there is no leakage in the remainder and a certain leakage in the aerosol. The nebulization process will alter the leakage in the remainder, on one hand directly (for example alternating pressure against the fluid from the vibrating mesh) and on the other hand indirectly. (Lots of droplets in the air-jet and ultrasonic nebulizers are „recycled“ back into the remainder by the baffles due to a big size.) Thus the leakage in both, aerosol and remainder will rise with time. The running time of the nebulizer and thus the amount of liquid left in the remainder has probably big influence

on the leakage (little amount left - big leakage and vice versa). The leakage in the aerosol of the Optineb®-ir was higher than in the remainder. This might be due to preferential transport of small, non-encapsulated fluorophore over big liposomes. One indication was the low concentration of liposomes in the aerosol (in contrast to the other nebulizers) and a good transport efficiency of small molecules.

In this study the average leakage from F1 liposomes was very small and seemed to be nebulizer independent. In contrast, the leakage of F2 and F3 liposomes differed among the nebulizers. The difference concerning leakage among the formulations was largest for vibrating mesh nebulizers. Hence it seems that vibrating mesh nebulizers have a larger impact on the stability than other nebulizer types.

Recently two studies were conducted which compared different nebulizer types with each other:
Kleemann et al (2007) nebulized liposomes made of DPPC : cholesterol and liposomes with additional PEGylation. They enclosed carboxyfluorescein (CF) and determined its leakage. Leakage was approximately 30 % for liposomes without PEGylation and 50 % for liposomes with DPPE–PEG. They assume that PEGylation causes membrane defects and results in a lower phase transition temperature, which makes liposomes less stable [38].
Elhissi et al (2012) nebulized liposomes made of DPPC : cholesterol and compared them with ultradeformable liposomes. They measured the leakage of salbutamol sulfate, which was over 30 % for conventional liposomes [42].
In both studies the lowest disruption was achieved with a vibrating mesh nebulizer. This result cannot be confirmed. However, different vibrating mesh nebulizers were used in all studies. This makes results difficult to compare. Moreover leakage rates were smaller in my study (<10 % for DPPC : cholesterol liposomes), this might be due to smaller liposomes. Larger liposomes (Kleemann: 250-400 nm; Elhissi: 4-6 µm) are likely to be more affected by nebulization.

2.5.4 Comparison of the two vibrating mesh nebulizers

Both vibrating mesh nebulizers showed high liposome transport efficacies and similar leakage rates. Since nebulization with the M-neb® was only performed twice (n=2), results were not further analyzed.

3 Aerosol droplet size dependencies (experiment II)

3.1 Summary

In this experiment the influence of liposome surface properties and different NaCl concentrations on the aerosol droplet size were determined. The surface modifications of the liposomes had no influence on the aerosol droplet size. In contrast the NaCl concentration had an impact. Higher NaCl concentrations decreased the droplet size. All measured aerosol droplets were in the desired range between 1 and 5 µm.

3.2 Introduction

Deposition mechanisms. Deposition of aerosol droplets in the respiratory tract depends on three main mechanisms. Those are impaction, sedimentation and diffusion. Two further, minor mechanisms are interception and electrostatic forces. All mechanisms are depicted in figure 25.

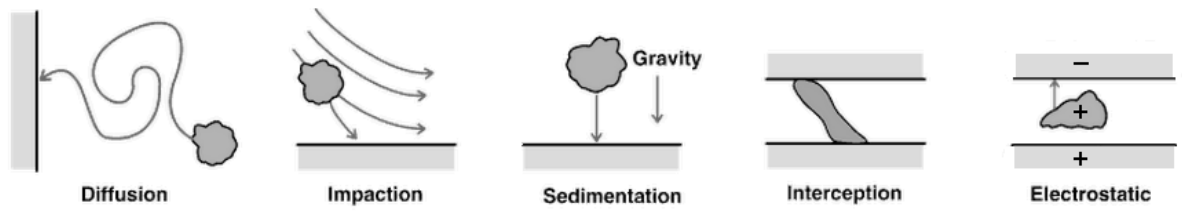

Figure 25: Mechanisms of droplet deposition [43].

Diffusion caused by Brownian motion leads to an attachment of the droplets to surrounding walls.
Impaction affects large droplets and means that those droplets have such a large momentum that they cannot follow the airflow when it changes direction. Large droplets are impacted at the upper airways.
Sedimentation means that droplets sink and deposit due to gravitational forces.
Sedimentation and diffusion happen mainly to small particles. Breathing pattern, individual anatomy of the lung (old person vs young person) and the aerosol droplet size generated by a nebulizer influence deposition [18].
Patients can reduce impaction if they inhale slowly. They can increase sedimentation of small particles when they inhale deeply and hold breath.

Aerosol droplet size. The aerosol droplet size is influenced by the nebulizer itself and physical properties of the formulation, mainly surface tension, viscosity, and ion concentration [30, 44, 45]. Temperature and air humidity influence the physical properties. Shortly after atomization water evaporates into the air, depending on temperature and air humidity. Evaporation decreases the aerosol droplet size and increases the lipid and ion concentrations in the remaining droplet [26].
With a shift in the aerosol droplet size, the place of deposition in the respiratory tract can be influenced. The human respiratory tract and the droplet deposition distribution therein are shown in the figures 26 and 27. Liposomes, which need to be deposited in the

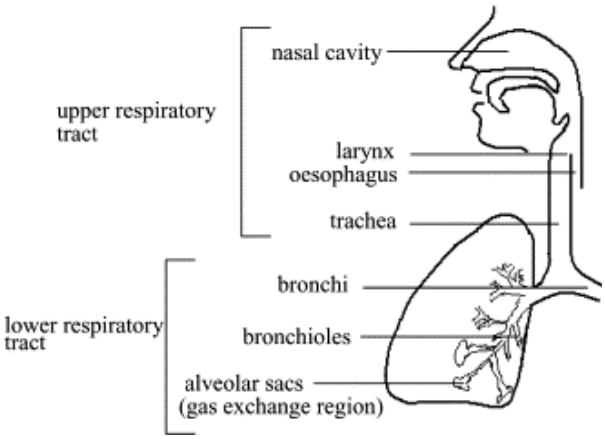

Figure 26: Anatomy of the human respiratory tract. The gas exchange happens in the alveoli, which outcrop from alveolar sacs [46].

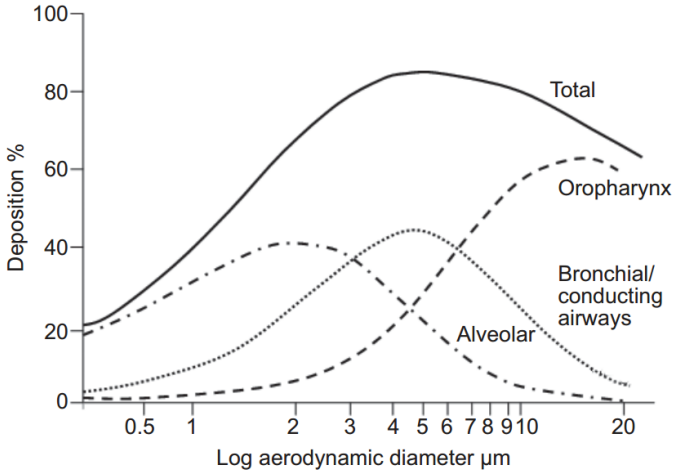

Figure 27: The relationship between aerodynamic diameter and lung deposition [23, 47].

lower lungs, have to be transported in aersosol droplets with sizes below 5 µm [18, 19].

Influence of viscosity. Viscosity influences the liquid flow rate which influences the aerosol droplet size slightly [44, 48]. The holes in the membrane of vibrating mesh nebulizers and the capillary fluid feeding tube in air-jet nebulizers can be approximated with a cylindrical tube. The fluid flow rate through those tubes can be calculated with Peuseuille's law (equation 11). The assumption is that the flow is laminar and the fluid is Newtonian.

$$Q = \frac{\pi \Delta P r^4}{8 \eta l} \tag{11}$$

Where r and l are radius and length of the tube, ΔP is the pressure drop, and η is the viscosity of the fluid. Thus the output is supposed to get less for higher viscous fluids [30].

Influence of surface tension. The surface tension of a fluid can be measured with a stalagmometer. A stalagmometer is basically a capillary glass tube which is open at the bottom. The fluid falls out in the shape of drops at the bottom, when the drops reach a certain size. The drop detaches, when its weight equals the circumference of the tube multiplied with the surface tension (equation 12) [30].

$$\rho V_\mathrm{d} g = 2\pi R \gamma \tag{12}$$

Where V_d is the volume of the drop, ρ is the density, and g is the gravitational acceleration. Thus a higher surface tension should yield to larger aerosol droplets. However, concerning nebulizers, findings have been conflicting [25].

Influence of ion concentration. Liquids build an electric double layer, when adjacent to a charged surface (for example the charged mesh aperture). While the liquid flows, the equilibrium ion concentration distribution gets perturbed. This perturbation produces an electric potential difference, and thus a resistance which opposes the flow. The magnitude of the resistance to the flow can be related to the thickness of the electric double layer, which is characterized by the Debye length λ_D, given in equation 13 [30].

$$\lambda_\mathrm{D} = \sqrt{\frac{\epsilon_\mathrm{r} \epsilon_0 k T}{\sum (z_\mathrm{i} e)^2 c_\mathrm{i}}} \tag{13}$$

Where ϵ_r is the relative permittivity of the solution, ϵ_o is the permittivity of vacuum, k is the Boltzmann constant, T is the absolute temperature, e is the elementary charge, z_i is the valency of the i^{th} ion, and c_i is the concentration in molecules/m^3.

The Debye length for NaCl in water at 25 °C is given in equation 14 [2]:

$$\lambda_{\mathrm{D}} = \frac{0.304}{\sqrt{c_{\mathrm{NaCl}}}} \tag{14}$$

Where c_{NaCl} is the NaCl concentration in mol/l. For example the Debye length of a 140 mM NaCl solution at 25 °C is approximately 0.81 nm. The Debye length of distilled water is a few 100 nm (due to impurities) [2]. Since distilled water has a higher Debye length than saline solutions, the nebulizer output of distilled water is supposed to be lower than the output of saline solutions.

The addition of an alkali halide salt (for example NaCl) to water inhibits bubble coalescence (it is the joining of two bubbles, getting one bubble). Hence this might lead to smaller droplets. The inhibition of coalescence can be explained with the ion distributions at the air/water interface. Polarizable ions like Cl^- show a propensity to the air/water surface, due to specific ion effects and polarization. Nonpolarizable ions like Na^+ prefer the aqueous bulk [48].

Mass Median Aerodynamic Diameter (MMAD). Every nebulizer has to be tested in vitro before market launch. Among others the MMAD of droplets and its Geometric Standard Deviation (GSD) have to be specified according to the ISO 27427, the EN 13544-1 and the „Guideline on the pharmaceutical Quality of Inhalation and Nasal Products, Health Canada/ EMEA“ [49]. The MMAD is the diameter of a droplet, such that half of the mass is contained in smaller droplets and half in larger droplets. The MMAD refers to particles in airflow, in contrast to the Mass Median Diameter (MMD). The MMAD can be determined by an impinger, an impactor or by laser diffraction [25]. Usually the MMAD and the MMD are identical.

3.3 Methods

3.3.1 Experiment design

Formulations. First the effect of the different formulations on the aerosol droplet size was determined. The procedure which follows was performed at least twice with each nebulizer:

1. Preparation of the three different liposomal formulations without ANTS/DPX. (see chapter 2.3.3)
2. Determination of the lipid concentration (see chapter 2.3.5) and dilution to 1 mg/ml.
3. Measurement of the aerosol droplet size. (see chapter 3.3.2)

NaCl. When there was evidence that NaCl influences the aerosol droplet size significantly, HEPES buffer with different concentrations of NaCl was nebulized with each nebulizer. (10 mM HEPES; pH 7.4; 0 mM NaCl, 70 mM NaCl, or 140 mM NaCl) The aerosol droplet size measurements (buffer with NaCl) were conducted three times with all four nebulizers. All measurements and the corresponding results are listed in the appendix.

3.3.2 Aerosol droplet size measurement

The aerosol droplet size was measured via laser diffraction with a Mastersizer 2000 (Malvern, Herrenberg, Germany). The analysis model name was „General purpose-fine“ and the dispersant name was „Water droplets“. The later had a refractive index of 1.33 and an absorption of 0.01. Measurements were carried out at a laser obscuration between 4 and 6 % at approximately 23 °C. The distance of the nebulizers to the Mastersizer depended on the intrinsic air flow rates. 3 ml probe were filled into the liquid reservoir and nebulized. Measurement was started after approximately 1 minute. Measurements were conducted at different days with freshly prepared liposomal suspensions or buffers. The result from the aerosol droplet size measurement is given as span and MMD.
The span is a measure for the broadness of the aerosol droplet size distribution and calculated with equation 15:

$$span = \frac{d(0.9) - d(0.1)}{d(0.5)} \tag{15}$$

d(0.1)	diameter, 10 % of the mass is in particles with a smaller diameter.
d(0.5)	diameter, 50 % of the mass is in particles with a smaller diameter.
d(0.9)	diameter, 90 % of the mass is in particles with a smaller diameter.

3.3.3 Statistical analysis

A **one-way ANOVA** was applied for aerosol droplet size analysis (parameter = NaCl concentration or formulation).
If the one-way ANOVA showed differences between the groups, 3 student's **t-tests with same variances** were used to compare the three groups with each other. A Bonferroni correction was made ($\alpha' = \alpha/3$) and a group was considered to be either bigger or smaller if the one tailed p-value (p') was below α'.
Statistical analysis was done with Microsoft Excel 2010.

3.4 Results

3.4.1 Influence of the surface modifications

The liposomal formulations had no impact on the aerosol droplet size, as depicted in figure 28. This was the case for all nebulizers, thus just one graph is shown (eFlow® rapid). The results for the other nebulizers are listed in the appendix.

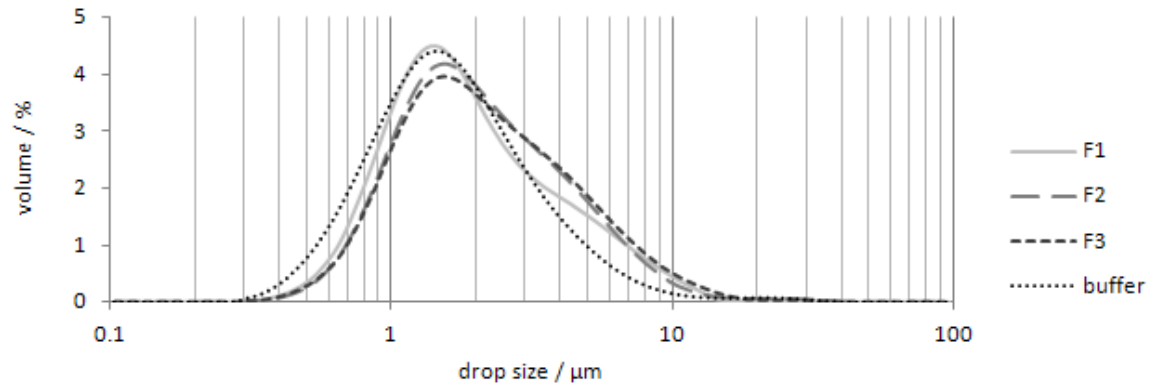

Figure 28: The presence of 1 mg/ml F1, F2, or F3 liposomes in the buffer did not affect its aerosol droplet size (p=0.29>α). (Buffer: 10 mM HEPES, pH 7.4, 140 mM NaCl; n=3; eFlow® rapid)

3.4.2 Influence of NaCl concentration

eFlow® rapid. Figure 29 shows, that the aerosol droplet size of 10 mM HEPES buffer (pH 7.4) nebulized with the eFlow® rapid decreased with higher concentrations of NaCl. A concentration of 140 mM NaCl yielded to significant smaller droplets than 0 mM NaCl (p'=0.001<α').

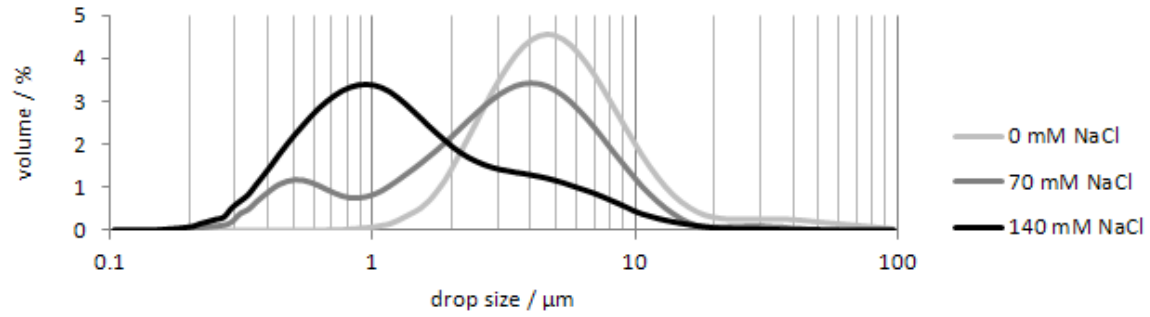

Figure 29: Aerosol droplet size with different concentrations of NaCl: eFlow® rapid; n=3; (buffer: 10 mM HEPES, pH 7.4)

NaCl decreased the aerosol droplet size of TRIS buffer and water too. Table 9 in the appendix gives an overview over the measurements conducted with all nebulizers and the corresponding aerosol droplet sizes and distributions.

MicroDrop MasterJet®. A 140 mM NaCl ($p'<0.001<\alpha'$) and a 70 mM NaCl ($p'=0.007<\alpha'$) concentration in the 10 mM HEPES buffer (pH 7.4) caused smaller aerosol droplets than a 0 mM NaCl concentration, when nebulized with the MicroDrop MasterJet® (figure 30).

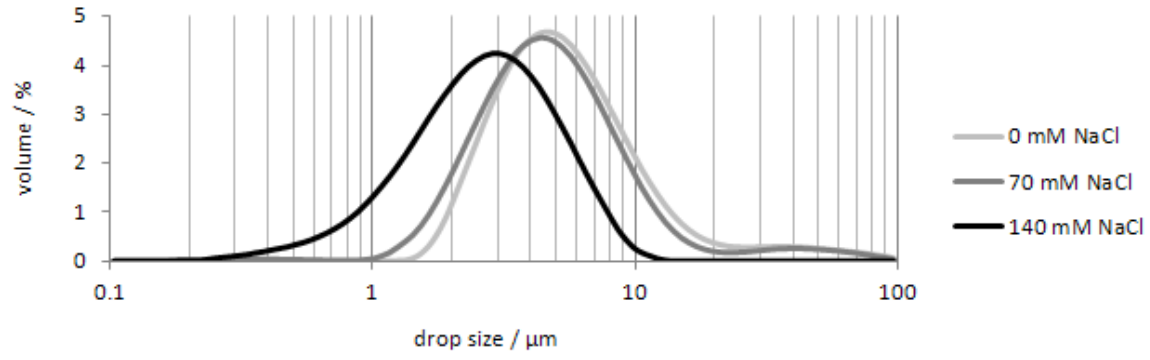

Figure 30: Aerosol droplet size with different concentrations of NaCl: MicroDrop MasterJet®; n=3; (buffer: 10 mM HEPES, pH 7.4)

Optineb®-ir. The different NaCl concentrations (0, 70, 140 mM) in the 10 mM HEPES buffer (pH 7.4) did not cause a significant difference (p=0.09>α) in the aerosol droplet size, when nebulized with the Optineb®-ir (figure 31).

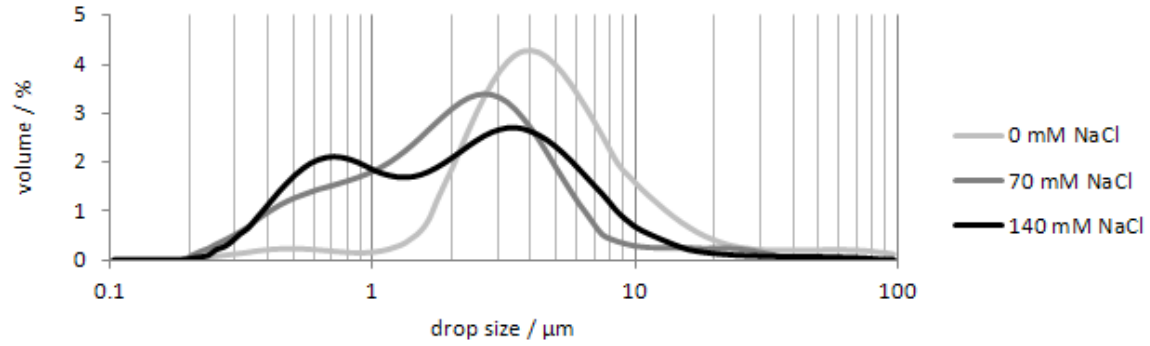

Figure 31: Aerosol droplet size with different concentrations of NaCl: Optineb®-ir; blue baffle plate; n=3; (buffer: 10 mM HEPES, pH 7.4)

M-neb®. A 140 mM NaCl concentration (p'<0.001<α') and a 70 mM NaCl concentration (p'<0.001<α') in 10 mM HEPES buffer (pH 7.4) caused smaller aerosol droplets than a 0 mM NaCl concentration, when nebulized with the M-neb® (figure 32).

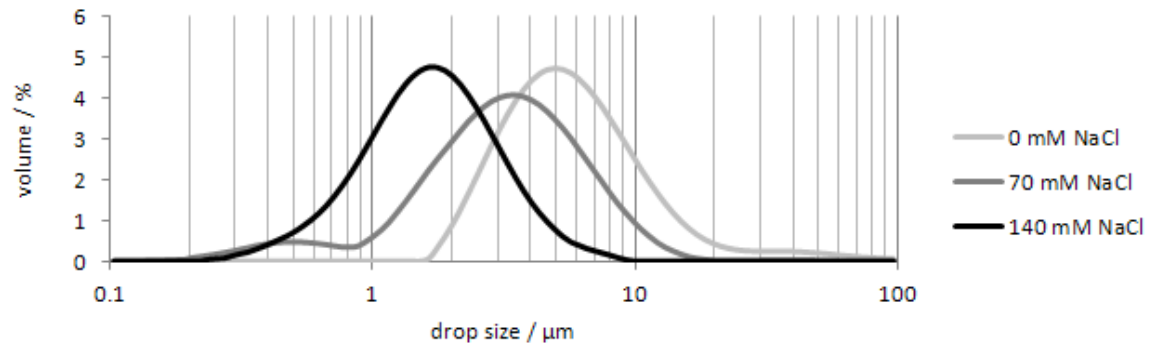

Figure 32: Aerosol droplet size with different concentrations of NaCl: M-neb®; n=3; (buffer: 10 mM HEPES, pH 7.4)

3.5 Discussion

The aerosol droplet size of HEPES buffer without NaCl was approximately the same (4-5 µm) for all four nebulizers. This size is comparable with previous findings and in the desired range [26, 30, 50]. In a recent study from Beck-Broichsitter et al (2014) the diameter of droplets nebulized with the eFlow® rapid fell from approximately 9 to 4 µm, when NaCl was added [48].

The intrinsic airflow rate of the ultrasonic nebulizer was not high enough for a measurement. Thus air flow was orally enhanced. This might have caused the vague results. The output per time was not determined during the aerosol droplet size measurement, but the output was visibly less for water and buffer without NaCl. This was already reported elsewhere [30, 45]. Broichsitter et al (2014) reported an increasing output and an increasing number of droplets emitted per second, when NaCl is added [48].

Viscosity stays nearly the same for low liposomal concentrations. This is probably why there was no difference concerning the aerosol droplet size between buffer and liposomal suspensions. Small NaCl concentrations do not change the viscosity either, but increase surface tension slightly [45]. Mc Callion et al (1995) nebulized fluids with different surface tension and found a small inverse correlation between surface tension and size [51]. Nevertheless there are a lot of conflicting results concerning the relation between surface tension and aerosol droplet size [18]. It is probably the ions which have a huge impact on size [30, 48, 52]. As mentioned before, the addition of NaCl inhibits bubble coalescence [52]. The air-jet and the ultrasonic nebulizer use a baffle plate to recycle droplets which are too large. Since the vibrating mesh nebulizers do not use a baffle plate, the addition of NaCl might have a bigger influence on the final droplet size for the vibrating mesh nebulizers.

The tested 140 mM NaCl concentration is slightly below physiological (154 mM). Most inhalation solutions have a physiological saline concentration, among others because hypertonic solutions cause bronchoconstriction [26].

4 Stability of liposomes in Alveofact® (experiment III)

4.1 Summary

In this experiment liposomes were incubated in pulmonary surfactant, in order to determine the influence of the surface modifications on stability. All liposomes were stable in Alveofact® over the (measured) time period of one hour.

4.2 Introduction

Surfactant. Pulmonary surfactant (short form of **surf**ace **act**ive **a**ge**nt**) consists of approximately 80 % phospholipids, 8 % neutral lipids (cholesterol and free fatty acids) and 12 % proteins. The surfactant adsorbs to the air-liquid interface in the small airways and the alveoli and reduces the surface tension. The internal pressure in the small airways is proportional to the surface tension and indirect proportional to the radius, according to Laplace's law shown in equation 16.

$$p = \frac{\gamma}{r} \tag{16}$$

Where p is the internal pressure, γ is the surface tension and r is the radius of the vessel. The pulmonary surfactant reduces the pressure which is needed to open small vessels after exhalation. Pressure is also reduced to open small alveoli, which can be approximated as spheres ($p = 2\gamma/r$). Laplace's law and the properties of the pulmonary surfactant help to explain the mechanics. However, a whole reduction to Laplace's law would be an oversimplification [53].

The pulmonary surfactant furthermore protects from injuries and infections. It is produced by type II pneumocytes [54].

Alveofact®. Alveofact® is a natural lung surfactant from bovine. It is isolated from bovine lung lavage and then prepared by lipid extraction and precipitation steps. Those essentially remove hydrophilic proteins, including surfactant apoprotein A (SP-A) [55]. The resulting phospholipid concentration is 41.7 mg/ml and the surfactant protein content is approximately 1 % SP-B & SP-C [56]. SP-B and SP-C are important for adsorption and spreading of the surfactant [54].

4.3 Materials and methods

4.3.1 Experiment design

The experiment was as follows:

1. Preparation of the three different liposomal formulations. (see chapter 2.3.3)
2. Separation of liposomes from non-encapsulated fluorophore. (see chapter 2.3.4)
3. Measurement of the lipid concentration (see chapter 2.3.5) and dilution to 1 mg/ml.
4. Dilution of Alveofact® with HEPES buffer (10 mM HEPES, 140 mM NaCl, pH 7.4) to a concentration of 0.5 mg/ml.
5. Measurement of the fluorescence intensity of Alveofact® (0.5 mg/ml). (see chapter 4.3.3)
6. Addition of liposomes to diluted Alveofact®. (see chapter 4.3.3)
7. Measurement of the fluorescence intensity over a time period of one hour. (see chapter 4.3.3)

4.3.2 Materials

Alveofact® was a gift from Lyomark (Oberhaching, Germany). For the other materials see chapter 2.3.2.

4.3.3 Fluorescence intensity measurement

Excitation and emission wavelength filter were set to 360 nm and 530 nm respectively. The time settings are shown in table 7.

Table 7: Time settings for fluorescence measurements in experiment III.

	without Triton X-100™			after addition of Triton X-100™		
	$t_{integration}$ s	$t_{repetition}$ s	t_{total} s	$t_{integration}$ s	$t_{repetition}$ s	t_{total} s
Fluorescence intensity	0.5	180	3600	0.1	2	60

Measurements were conducted with an 105.253-QS 10 x 2 mm quartz cuvette at a temperature of 37 °C. 5 µl probe with a lipid concentration of 1 mg/ml was diluted in 200 µl Alveofact® (0.5 mg/ml). After addition of 2 µl 10% Triton X-100™ the measurement was repeated with the time settings given in table 7.

4.4 Results

Alveofact® has a broad emission spectrum and thus showed a high auto-fluorescence. After addition of Triton X-100™ fluorescence intensity of Alveofact® decreased in contrast to the fluorescence intensity of liposomes which released the loaded fluorophore. The background fluorescence of Alveofact® was subtracted from the overall fluorescence intensity of liposomes in Alveofact®. The result is shown in figure 33.

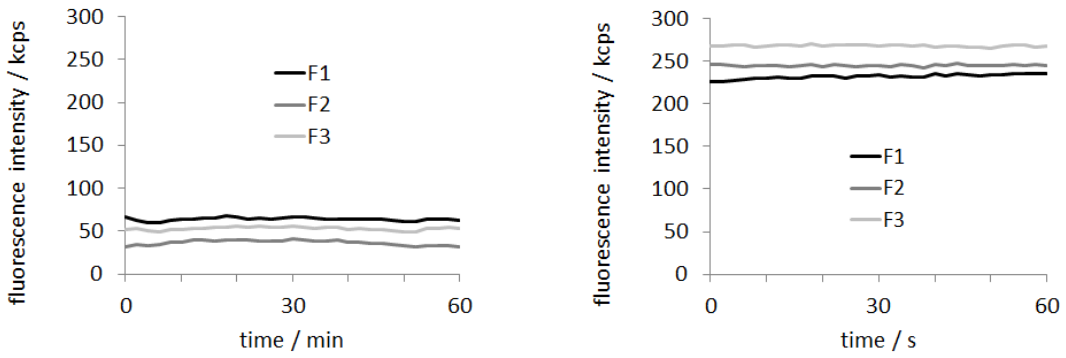

(a) without Triton X-100™ (b) with Triton X-100™

Figure 33: Time behavior of fluorescence intensity for the different, fluorophore loaded, liposomal formulations in the lung surfactant Alveofact® (a). After one hour, Triton X-100™ was added. The fluorescence intensities after the addition of Triton X-100™ are shown in (b). (n=1)

4.5 Discussion

Anabousi et al (2006) reported that PEGylation reduces long term leakage of calcein from transferrin conjugated DPPC : cholesterol liposomes in Alveofact® [57].
As shown in fig 33 all three liposomal formulations (F1, F2, F3) were stable in Alveofact®, regardless of the PEGylation. The results are comparable with a study from Abu-Dahab et al (2001) [58]. Therein DPPC : cholesterol liposomes in Alveofact® showed hardly any leakage over a time period of 6 hours. Nevertheless there might be leakage for a longer time period.
Freshly prepared liposomes were used, because nebulization with three different nebulizers would have tripled the number of probes. Already nebulized liposomes might have higher leakage rates in Alveofact® than non-nebulized samples. However the experiment was performed once and has to be repeated before any clear conclusion can be drawn.

5 Conclusion

The main findings of this study are as follows.

- Liposome transport efficacy depends on the nebulizer principle.
- The vibrating mesh technology is the most efficient aerosolization technique.
- Liposome stability during nebulization depends mainly on the liposome surface modification/formulation.
- The inclusion of DPPE–PEG_{2000} and DOTAP makes DPPC : cholesterol liposomes less stable and leakier.
- PDI and leakage are positively correlated.

- Low ($\approx 1\,\mathrm{mg/ml}$) lipid concentrations of liposomal suspensions and small surface modifications do not influence the aerosol droplet size.
- The addition of NaCl to the liposome buffer strongly decreases the aerosol droplet size.

- Tested liposomes are stable in Alveofact® over a time period of one hour.

Taken together, the author concludes that the vibrating mesh technique is very promising for liposome inhalation therapy, due to its high liposome transport efficacy. Future studies will probably focus on the vibrating mesh nebulizers and on liposomal formulations suitable for vibrating mesh nebulizers.

References

[1] Riaz M: Liposomes preparation methods. *Pak J Pharm Sci* 9: 65–77 (1996)

[2] Alberts B et al. *Molecular Biology of the Cell.* New York, Garland Science (2002)

[3] Chang HI, Yeh MK: Clinical development of liposome-based drugs: formulation, characterization, and therapeutic efficacy. *Int J Nanomedicine* 7: 49–60 (2012)

[4] Cipolla D, Gonda I, Chan HK: Liposomal formulations for inhalation. *Ther Deliv* 4: 1047–1072 (2013)

[5] Roberts MJ, Bentley MD, Harris JM: Chemistry for peptide and protein PEGylation. *Adv Drug Deliv Rev* 54: 459–476 (2002)

[6] Roche Diagnostics: DOTAP Liposomal Transfection Reagent. *Ref. 11202375001* (2011) URL: www.cssportal.roche.com/LFR_PublicDocs/ras/11202375001_en_12.pdf

[7] Madhongsa K et al.: Antimicrobial Action of the Cyclic Peptide Bactenecin on Burkholderia pseudomallei Correlates with Efficient Membrane Permeabilization. *PLoS Negl Trop Dis* 7: e2267 (2013)

[8] Frederick TE et al.: Bis(monoacylglycero)phosphate forms stable small lamellar vesicle structures: insights into vesicular body formation in endosomes. *Biophys. J.* 96: 1847–1855 (2009)

[9] Lange S et al.: Interaction of earthworm hemolysin with lipid membranes requires sphingolipids. *J. Biol. Chem.* 272: 20884–20892 (1997)

[10] Tokarska-Schlattner M et al.: Phosphocreatine interacts with phospholipids, affects membrane properties and exerts membrane-protective effects. *PLoS ONE* 7: e43178 (2012)

[11] Ladokhin AS, Wimley WC, White SH: Leakage of membrane vesicle contents: determination of mechanism using fluorescence requenching. *Biophys. J.* 69: 1964–1971 (1995)

[12] Rodnin MV et al.: Interactions of fluorinated surfactants with diphtheria toxin T-domain: testing new media for studies of membrane proteins. *Biophys. J.* 94: 4348–4357 (2008)

[13] Shnyrova AV, Zimmerberg J: Chapter 4 - Reconstitution of membrane budding with unilamellar vesicles. *Meth. Enzymol.* 464: 55–75 (2009)

[14] Ahyayauch H et al.: Effects of chronic and acute lead treatments on the biophysical properties of erythrocyte membranes, and a comparison with model membranes. *FEBS Open Bio* 3: 212–217 (2013)

[15] Palchevskyy SS et al.: Chaperoning of insertion of membrane proteins into lipid bilayers by hemifluorinated surfactants: application to diphtheria toxin. *Biochemistry* 45: 2629–2635 (2006)

[16] Needham D: Temperature-sensitive liposomal formulation. *Patent WO/1999/065466* (1999)

[17] ANTS/DPX Assay. *Encapsula Nanosciences* (2012) URL: www.fluoroliposome.com/intermixing-of-aqueous-contents/antsdpx-assay/

[18] Boe J et al.: European Respiratory Society Guidelines on the use of nebulizers Guidelines prepared by a European Respiratory Society Task Force on the use of nebulizers. *European Respiratory Journal* 18: 228–242 (2001)

[19] Shah ND, Shah VV, Chivate ND: Pulmonary Drug Delivery: A Promising Approach. *Journal of Applied Pharmaceutical Science* 2: 33–37 (2012)

[20] Praveen Buddiga MD: Use of Metered Dose Inhalers, Spacers, and Nebulizers. *Medscape* (2013) URL: http://emedicine.medscape.com/article/1413366-overview#aw2aab6b3

[21] Newman SP: Principles of metered-dose inhaler design. *Respiratory care* 50: 1177–1190 (2005)

[22] Geller DE: Comparing clinical features of the nebulizer, metered-dose inhaler, and dry powder inhaler. *Respiratory care* 50: 1313–1322 (2005)

[23] Laube BL et al.: What the pulmonary specialist should know about the new inhalation therapies. *European Respiratory Journal* 37: 1308–1417 (2011)

[24] Nikander K, Sanders M: The early evolution of nebulizers. *Medicamundi* 54: 47–53 (2010)

[25] O'Callaghan C, Barry PW: The science of nebulised drug delivery. *Thorax* 52 Suppl 2: 31–44 (1997)

[26] Phipps PR, Gonda I: Droplets produced by medical nebulizers Some factors affecting their size and solute concentration. *Chest* 97: 1327–1332 (1990)

[27] Yeo LY et al.: Ultrasonic nebulization platforms for pulmonary drug delivery. *Expert Opin Drug Deliv* 7: 663–679 (2010)

[28] Vecellio L: The mesh nebuliser: a recent technical innovation for aerosol delivery. *Breathe* 2: 252–260 (2006)

[29] Nebu-Tec: Instructions for use: VENTA-NEB-ir. *Manual* (2013) URL: http://www.nebu-tec.de/nt/pdf/NT_ON-100-4_IFU_Venta-Neb-D_A.pdf

[30] Zhang G, David A, Wiedmann TS: Performance of the vibrating membrane aerosol generation device: Aeroneb Micropump Nebulizer. *J Aerosol Med* 20: 408–416 (2007)

[31] Humberstone VC et al.: Fluid droplets production apparatus and method. *Patent WO/1993/010910* (1993)

[32] Humberstone VC, Ross CJ: Dispensing apparatus having a perforate outlet member and a vibrating device. *US Patent Nr. 5152456* (1992)

[33] PARI Pharma GmbH: Instructions for use: eFlow rapid nebulizer system. *Manual*: 41 (2012) URL: http://www.pari.de/fileadmin/user_upload/Documents/PARI_Germany/Instruction-for-use/Compressor/178D1007-eFlow-rapid-WE.pdf

[34] Gallem T et al.: Inhalation nebulizer. *US Patent Nr. 6962151* (2005)

[35] Sant AJ et al.: Liquid supply apparatus. *Patent WO/1997/029851* (1997)

[36] Gallem T, Ulrich M: Aerosol generator. *Patent WO/2002/064265* (2002)

[37] Dolovich MB, Dhand R: Aerosol drug delivery: developments in device design and clinical use. *Lancet* 377: 1032–1045 (2011)

[38] Kleemann E et al.: Iloprost-containing liposomes for aerosol application in pulmonary arterial hypertension: formulation aspects and stability. *Pharm Res* 24: 277–287 (2007)

[39] DiaSys Diagnostics System GmbH: Phospholipids FS. *Manual* (2008)

[40] Cinelli S et al.: Properties of mixed DOTAP-DPPC bilayer membranes as reported by differential scanning calorimetry and dynamic light scattering measurements. *J Phys Chem B* 111: 10032–10039 (2007)

[41] Tieleman DP et al.: Simulation of pore formation in lipid bilayers by mechanical stress and electric fields. *J. Am. Chem. Soc.* 125: 6382–6383 (2003)

[42] Elhissi AM et al.: Nebulization of ultradeformable liposomes: the influence of aerosolization mechanism and formulation excipients. *Int J Pharm* 436: 519–526 (2012)

[43] Scott B: Deposition of Radioactive Substances in the Respiratory Tract. (2009) URL: www.radiation-scott.org/deposition/particles.htm

[44] Mc Callion ONM et al.: Nebulization of fluids of different physicochemical properties with air-jet and ultrasonic nebulizers. *Pharmaceutical research* 12: 1682–1688 (1995)

[45] Ghazanfari T et al.: The influence of fluid physicochemical properties on vibrating-mesh nebulization. *International journal of pharmaceutics* 339: 103–111 (2007)

[46] Hussain A et al.: Absorption enhancers in pulmonary protein delivery. *J Control Release* 94: 15–24 (2004)

[47] Koebrich R, Rudolf G, Stahlhofen W A: A mathematical model of mass deposition in man. *Ann Occup Hyg*: 15–23 (1994)

[48] Beck-Broichsitter M et al.: On the correlation of output rate and aerodynamic characteristics in vibrating-mesh-based aqueous aerosol delivery. *Int J Pharm* 461: 34–37 (2014)

[49] Copley M: Nebulizer testing. *Inhalation CSC publishing, St Paul, MN*: 31–34 (2008)

[50] Steckel H, Eskandar F: Factors affecting aerosol performance during nebulization with jet and ultrasonic nebulizers. *Eur J Pharm Sci* 19: 443–455 (2003)

[51] Mc Callion ONM et al.: The influence of surface tension on aerosols produced by medical nebulisers. *International journal of pharmaceutics* 129: 123–136 (1996)

[52] Jungwirth P, Tobias DJ: Specific ion effects at the air/water interface. *Chemical Reviews* 106: 1259–1281 (2006)

[53] Prange HD: Laplace's law and the alveolus: a misconception of anatomy and a misapplication of physics. *Adv Physiol Educ* 27: 34–40 (2003)

[54] Saxena S: Lung surfactant. *Resonance* 10: 91–96 (2005)

[55] Bernhard W et al.: Commercial versus native surfactants Surface activity, molecular components, and the effect of calcium. *Am J Respir Crit Care Med* 162: 1524–1533 (2000)

[56] Fox GF, Sothinathan U: The choice of surfactant for treatment of respiratory distress syndrome in preterm infants: A review of the evidence. *Infant* 1: 8–12 (2005)

[57] Anabousi S et al.: Effect of PEGylation on the stability of liposomes during nebulisation and in lung surfactant. *J Nanosci NaJournalchnol* 6: 3010–3016 (2006)

[58] Abu-Dahab R, Schafer UF, Lehr CM: Lectin-functionalized liposomes for pulmonary drug delivery: effect of nebulization on stability and bioadhesion. *Eur J Pharm Sci* 14: 37–46 (2001)

[59] MPV Truma: Atmen ist Leben. *Manual* (2003) URL: http://www.mpv-truma.com/downloads/products/MicroDrop_de_eng.pdf

All URLs were visited on August 12, 2013.

Appendix

Table 8 and 9 show several measured droplet sizes. HEPES buffer (10 mM Hepes, pH 7.4) with 140 mM NaCl was nebulized in both sub-experiments, in the experiment which tested the influence of liposomes (marked with (*) in the tables) and in the experiment which tested the influence of different NaCl concentrations (**). All ingredients were added to bidistilled water.

Table 10 shows the technical data of the nebulizers.

Table 8: MMD and span of aerosol droplets generated with M-neb® and eFlow® rapid. (mean ± SD)

	MMD µm	span µm	n 1
a) M-neb®			
0 mM NaCl, 10 mM HEPES, pH 7.4	5.51 ± 0.28	1.88 ± 0.38	2
0 mM NaCl	5.09 ± 0.14	1.61 ± 0.44	2
0 mM NaCl, 10 mM TRIS, pH 7.4	5.08	1.42	1
70 mM NaCl, 10 mM HEPES, pH 7.4	3.47 ± 0.92	1.61 ± 0.29	2
140 mM NaCl	3.08 ± 0.87	1.52 ± 0.14	2
154 mM NaCl	2.05	2.19	1
140 mM NaCl, 10 mM HEPES, pH 7.4	1.70 ± 0.02	1.54 ± 0.34	2
154 mM NaCl, 10 mM TRIS, pH 7.4	1.06	2.68	1
b) eFlow® rapid			
0 mM NaCl	5.28 ± 0.14	1.75 ± 0.40	2
0 mM NaCl, 10 mM HEPES, pH 7.4	4.91 ± 0.43	2.02 ± 0.51	3
140 mM NaCl	4.89 ± 0.85	2.40 ± 0.09	2
0 mM NaCl, 10 mM TRIS, pH 7.4	4.77	1.58	1
70 mM NaCl, 10 mM HEPES, pH 7.4	3.42 ± 1.09	1.71 ± 0.08	3
140 mM NaCl, 10 mM HEPES, pH 7.4, 1 mg/ml F3	2.32 ± 0.81	1.64 ± 0.45	3
140 mM NaCl, 10 mM HEPES, pH 7.4, 1 mg/ml F2	2.24 ± 0.81	1.55 ± 0.37	3
140 mM NaCl, 10 mM HEPES, pH 7.4, 1 mg/ml F1	2.12 ± 0.81	1.48 ± 0.37	3
154 mM NaCl	2.05	2.19	1
140 mM NaCl, 10 mM HEPES, pH 7.4, (*)	1.72 ± 0.40	1.61 ± 0.35	2
154 mM NaCl, 10 mM TRIS, pH 7.4	1.44	1.16	1
140 mM NaCl, 10 mM HEPES, pH 7.4, (**)	1.29 ± 0.61	4.64 ± 4.39	3
140 mM NaCl, 10 mM HEPES, pH 7.4, ANTS/DPX, F1	1.24	1.07	1
LipoAerosol®	0.85	0.10	1

Table 9: MMD and span of aerosol droplets generated with MicroDrop MasterJet® and Optineb®-ir. (mean ± SD)

	MMD µm	span µm	n 1
c) MicroDrop MasterJet®			
0 mM NaCl	5.49 ± 0.02	2.01 ± 0.60	2
154 mM NaCl	5.25	1.35	1
0 mM NaCl, 10 mM HEPES, pH 7.4	5.15 ± 0.07	2.12 ± 0.54	3
140 mM NaCl	4.95 ± 0.12	2.38 ± 0.61	2
0 mM NaCl, 10 mM TRIS, pH 7.4	4.86	1.41	1
70 mM NaCl, 10 mM HEPES, pH 7.4	4.57 ± 0.27	2.01 ± 0.47	3
140 mM NaCl, 10 mM HEPES, pH 7.4, 1 mg/ml F1	3.89 ± 0.14	2.55 ± 0.40	2
140 mM NaCl, 10 mM HEPES, pH 7.4, (*)	3.78 ± 0.47	2.60 ± 0.20	2
154 mM NaCl, 10 mM TRIS, pH 7.4	3.57	1.61	1
140 mM NaCl, 10 mM HEPES, pH 7.4, 1 mg/ml F3	3.42 ± 0.63	2.20 ± 0.13	2
140 mM NaCl, 10 mM HEPES, pH 7.4, ANTS/DPX, F1	3.41	2.02	1
140 mM NaCl, 10 mM HEPES, pH 7.4, 1 mg/ml F2	3.33 ± 0.76	2.51 ± 0.45	2
140 mM NaCl, 10 mM HEPES, pH 7.4, (**)	2.73 ± 0.35	1.65 ± 0.09	2
LipoAerosol®	2.69	2.15	1
d) Optineb®-ir			
LipoAerosol®	5.26	1.55	1
0 mM NaCl, 10 mM HEPES, pH 7.4	4.67 ± 1.20	2.23 ± 0.54	3
0 mM NaCl	4.39 ± 1.04	2.14 ± 0.71	2
140 mM NaCl, 10 mM HEPES, pH 7.4, 1 mg/ml F3	3.53 ± 1.27	2.31 ± 0.35	2
140 mM NaCl, 10 mM HEPES, pH 7.4, 1 mg/ml F2	3.21 ± 1.61	1.97 ± 0.42	2
140 mM NaCl, 10 mM HEPES, pH 7.4, 1 mg/ml F1	3.14 ± 1.89	2.27 ± 0.03	2
140 mM NaCl, 10 mM HEPES, pH 7.4, (*)	2.99 ± 1.63	2.10 ± 0.35	2
140 mM NaCl, 10 mM HEPES, pH 7.4, (**)	2.55 ± 1.38	2.62 ± 1.07	2
140 mM NaCl	2.28 ± 0.33	2.05 ± 0.02	2
70 mM NaCl, 10 mM HEPES, pH 7.4	2.08 ± 0.40	3.48 ± 2.06	3
154 mM NaCl	1.93	2.13	1

Table 10: Technical data of the nebulizers [29, 33, 59].

	eFlow® rapid	MicroDrop MasterJet®	Optineb®-ir	M-neb®
Model	178G1005	M51400-00		
Type	vibrating mesh	air-jet	ultrasonic	vibrating mesh
Operating mode	continuous	continuous	hubs	continuous or hubs
Size control (H x W x D)	40 x 116 x 116 mm	122 x 217 x 265 mm	105 x 66 x 98 mm	
Size handset (H x W x D)	63 x 50 x 145 mm	40 x 116 x 116 mm	-	
Weight	0.3 kg	2.5 kg	0.3 kg	
Battery	4 x 1.2 V (rechargeable) 4 x 1.5 V (disposable)	no	12 V (rechargeable)	
Power supply	100 – 240 V AC, 50-60 Hz	230 V AC, 50 Hz	120/240 V AC	
Operating power consumption	max. 2.5 W		max. 18 W	
Frequency/pressure	117 kHz	1.2 bar	2.4 MHz	115 kHz
Total output rate	500 mg/min	>400 mg/min	0.6 ml/min	
MMAD	4.1 µm	3 µm	2 µm	
Fill volume	2 – 6 ml		≤6 ml	
Electric protection class	II, BF	II, B	II, B	
Storage temperature	20 – 60 °C		-5 – 40 °C	
Operating temperature	15 – 35 °C		15 – 25 °C	
Operating air humidity	15 – 93 %		40 – 75 %	